Cell Reports
Medicine

Article

Ligand-mediated PAI-1 inhibition in a mouse model of peritoneal carcinomatosis

Graphical abstract

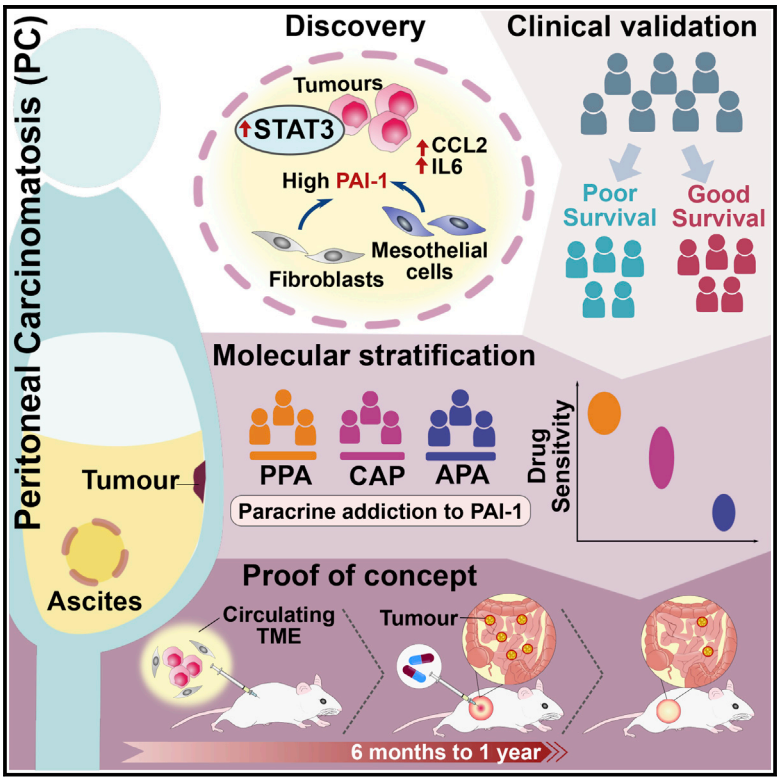

Highlights

- PAI-1 is a key STAT3 activating ligand in ascites and predicts patients' survival
- Single-cell analysis identifies fibroblasts as key secretors of PAI-1 into ascites
- PAI-1 and p-STAT3 molecular stratification predicts therapeutic efficacy
- PAI-1 inhibition is therapeutically effective in paracrine addicted PC mouse model

Authors

Josephine Hendrikson, Ying Liu, Wai Har Ng, ..., Melissa Ching Ching Teo, Chin-Ann J. Ong, on behalf of the Singapore Peritoneal Oncology Study (SPOS) Group and Singapore Gastric Cancer Consortium (SGCC)

Correspondence

johnny.ong.c.a@singhealth.com.sg

In brief

Hendrikson et al. demonstrate that a phenomenon of paracrine addiction in a closed biological system can be exploited for therapy following molecular stratification in peritoneal carcinomatosis. We present proof-of-concept experiments performed in patient-derived ascites-dependent xenografts targeting PAI-1, a key ligand secreted by fibroblasts and mesothelial cells into ascites.

Hendrikson et al., 2022, Cell Reports Medicine *3*, 100526
February 15, 2022
https://doi.org/10.1016/j.xcrm.2022.100526

CellPress

Cell Reports Medicine

CellPress
OPEN ACCESS

Article

Ligand-mediated PAI-1 inhibition in a mouse model of peritoneal carcinomatosis

Josephine Hendrikson,[1,2,3,20] Ying Liu,[1,2,3,20] Wai Har Ng,[1,2,3] Jing Yi Lee,[4] Abner Herbert Lim,[4] Jui Wan Loh,[4] Cedric C.Y. Ng,[5] Whee Sze Ong,[6] Joey Wee-Shan Tan,[1,2,3] Qiu Xuan Tan,[1,2,3] Gillian Ng,[1,2,3] Nicholas B. Shannon,[1,2,3] Weng Khong Lim,[7,8] Tony K.H. Lim,[9,10] Clarinda Chua,[11] Jolene Si Min Wong,[1,2,12,13] Grace Hwei Ching Tan,[1,2] Jimmy Bok Yan So,[14,15] Khay Guan Yeoh,[16,17] Bin Tean Teh,[5,18] Claramae Shulyn Chia,[1,2,12,13] Khee Chee Soo,[1,2] Oi Lian Kon,[3] Iain Beehuat Tan,[8,11,19] Jason Yongsheng Chan,[4,11] Melissa Ching Ching Teo,[1,2] Chin-Ann J. Ong,[1,2,3,12,13,18,21,22,23,*] and on behalf of the Singapore Peritoneal Oncology Study (SPOS) Group and Singapore Gastric Cancer Consortium (SGCC)

[1]Department of Sarcoma, Peritoneal and Rare Tumours (SPRinT), Division of Surgery and Surgical Oncology, National Cancer Centre Singapore, 11 Hospital Cresent, Singapore 169610, Singapore
[2]Department of Sarcoma, Peritoneal and Rare Tumours (SPRinT), Division of Surgery and Surgical Oncology, Singapore General Hospital, Singapore 169608, Singapore
[3]Laboratory of Applied Human Genetics, Division of Medical Sciences, National Cancer Centre Singapore, Singapore 169610, Singapore
[4]Cancer Discovery Hub, National Cancer Centre Singapore, Singapore 169610, Singapore
[5]Laboratory of Cancer Epigenome, Division of Medical Sciences, National Cancer Centre Singapore, Singapore 169610, Singapore
[6]Division of Clinical Trials and Epidemiological Sciences, National Cancer Centre Singapore, Singapore 169610, Singapore
[7]SingHealth Duke-NUS Institute of Precision Medicine, National Heart Centre Singapore, Singapore 169609, Singapore
[8]Cancer and Stem Biology Signature Research Program, Duke-NUS Medical School, Singapore 169857, Singapore
[9]Department of Anatomical Pathology, Singapore General Hospital, Singapore 169856, Singapore
[10]Pathology Academic Clinical Program, SingHealth Duke-NUS Academic Medical Centre, Singapore 168753, Singapore
[11]Division of Medical Oncology, National Cancer Centre Singapore, Singapore 169610, Singapore
[12]SingHealth Duke-NUS Oncology Academic Clinical Program, Duke-NUS Medical School, Singapore 169857, Singapore
[13]SingHealth Duke-NUS Surgery Academic Clinical Program, Duke-NUS Medical School, Singapore 169857, Singapore
[14]Department of Surgery, Yong Loo Lin School of Medicine, National University of Singapore, Singapore 119077, Singapore
[15]Division of Surgical Oncology, National University Cancer Institute, National University Health System, Singapore 119074, Singapore
[16]Department of Medicine, Yong Loo Lin School of Medicine, National University of Singapore, Singapore 119077, Singapore
[17]Department of Gastroenterology and Hepatology, National University Hospital, Singapore 119074, Singapore
[18]Institute of Molecular and Cell Biology, A*STAR Research Entities, Singapore 138673, Singapore
[19]Laboratory of Applied Cancer Genomics, Genome Institute of Singapore, A*STAR Research Entities, Singapore 138672, Singapore
[20]These authors contributed equally
[21]Twitter: @LaboratoryAHG
[22]Twitter: @JohnnyOngCA
[23]Lead contact
*Correspondence: johnny.ong.c.a@singhealth.com.sg
https://doi.org/10.1016/j.xcrm.2022.100526

SUMMARY

Peritoneal carcinomatosis (PC) present a ubiquitous clinical conundrum in all intra-abdominal malignancies. Via functional and transcriptomic experiments of ascites-treated PC cells, we identify STAT3 as a key signaling pathway. Integrative analysis of publicly available databases and correlation with clinical cohorts (n = 7,359) reveal putative clinically significant activating ligands of STAT3 signaling. We further validate a 3-biomarker prognostic panel in ascites independent of clinical covariates in a prospective study (n = 149). Via single-cell sequencing experiments, we uncover that PAI-1, a key component of the prognostic biomarker panel, is largely secreted by fibroblasts and mesothelial cells. Molecular stratification of ascites using PAI-1 levels and STAT3 activation in ascites-treated cells highlight a therapeutic opportunity based on a phenomenon of paracrine addiction. These results are recapitulated in patient-derived ascites-dependent xenografts. Here, we demonstrate therapeutic proof of concept of direct ligand inhibition of a prognostic target within an enclosed biological space.

INTRODUCTION

In many abdominopelvic malignancies, intraperitoneal dissemination culminates in a clinical condition known as peritoneal carcinomatosis (PC).[1] From a biological perspective, PC consists of distinct independent deposits of metastatic tumor bathed with ascitic fluid within the abdominal cavity. Characterizations of ascites proteome from ovarian PC and gastric PC

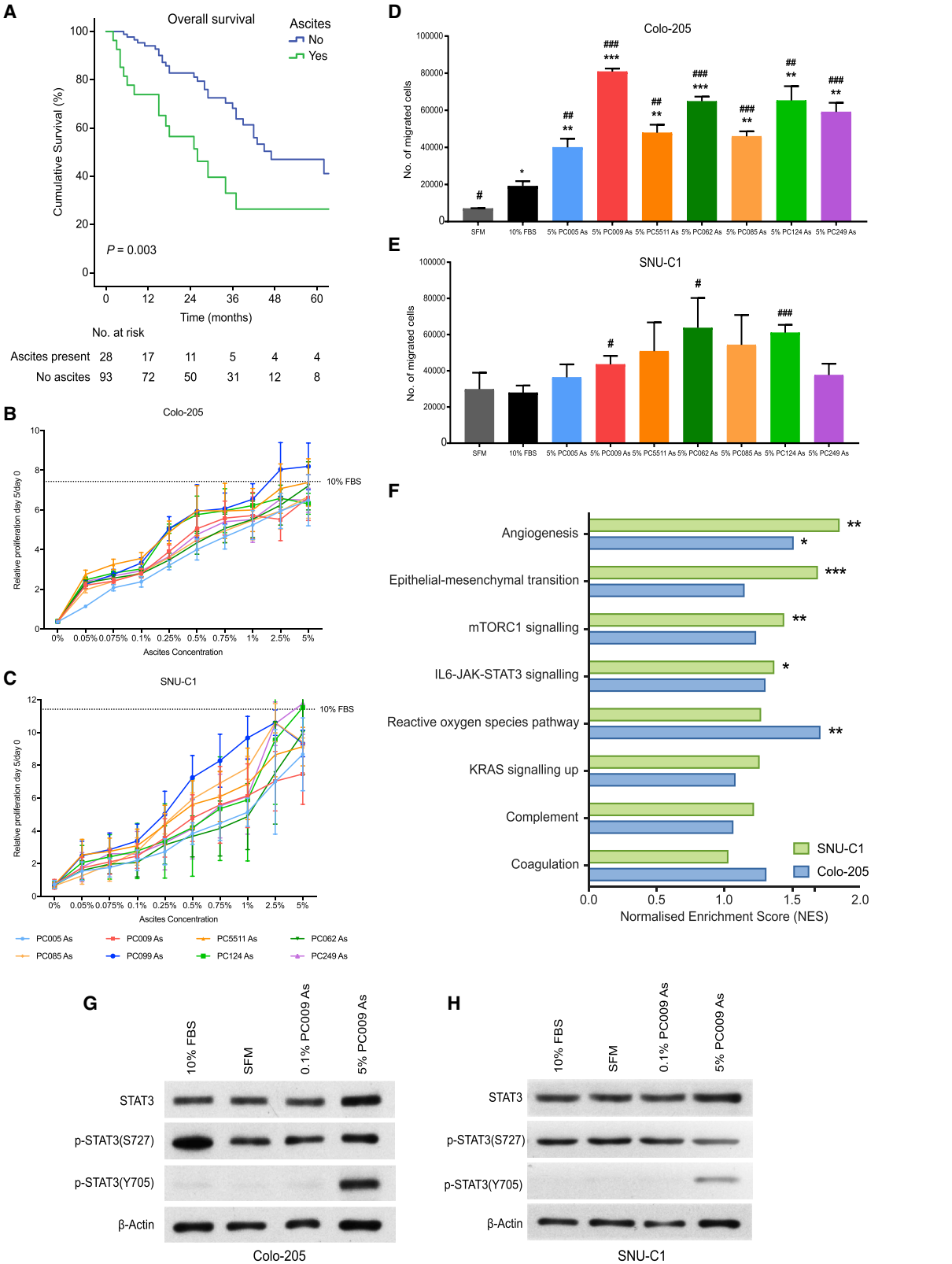

(legend on next page)

have demonstrated that ascites contains elevated pro-tumorigenic factors such as interleukin (IL)-6, IL-10, osteoprotegerin (OPG), vascular endothelial growth factor (VEGF), progastricsin (PGC) and periostin (POSTN).[2–6] VEGF, in particular, has been extensively studied in ovarian PC ascites and found to be an important mediator of ascites formation and metastasis through increased vascular permeability and neovascularization.[7,8] However, inhibition of VEGF has remained limited due to the lack of predictive biomarkers for therapeutic response and activation of resistance pathways.[9,10]

Reasoning that the composition of ascitic fluid might offer insight into the memory of key biological events occurring intra-abdominally, we hypothesized that paracrine factors essential for survival and growth of peritoneal deposits are secreted into and circulate within ascitic fluid. Extrapolating from this hypothesis, a logical assumption is that perturbation of a key paracrine factor necessary for survival of tumor cells and circulating within this tumor microenvironment could exploit the molecular addiction for successful therapy. Here, we set out to experimentally validate this approach of paracrine inhibition to treat PC.

RESULTS

Ascites in PC is clinically prognostic and biologically active

We first sought to evaluate if the presence of ascites in PC patients is clinically significant. Consistent with literature describing the prognostic significance of malignant ascites,[11] we observed that the presence of gross ascites in a cohort of 121 PC patients undergoing cytoreductive surgery (CRS) was linked to a much poorer overall survival (HR = 2.428, p = 0.003) (Figure 1A). Multivariate analysis demonstrated that the presence of ascites was the most significant clinical prognostic factor (p = 0.004) (Table S1). To assess the biological effects of ascites on cancer cells, we treated two colorectal cancer cell lines representative of PC (Colo-205 and SNU-C1) with cell-free ascites (CFA) originating from different patients diagnosed with colorectal cancer. The addition of CFA to serum-free medium (SFM) was sufficient to stimulate cellular proliferation in a dose-dependent fashion as well as induce migration of cancer cells (Figures 1B–1E). Together, the data suggest that ascites contains biologically active ligands capable of supporting cellular functions of cancer cells, thus potentially explaining their link to poor outcomes.

To decipher downstream signaling pathways activated in cancer cells when exposed to ascites, we performed gene expression analysis of Colo-205 and SNU-C1 cells upon exposure to PC ascites. RNA microarray analysis of Colo-205 and SNU-C1 cells exposed to 5% CFA (by volume) showed enrichment of signatures representing angiogenesis and epithelial-mesenchymal transition (EMT) along with upregulation of mTORC1 and STAT3 signaling (Figure 1F). STAT3 signaling, in particular, is of interest because it has been reported as an integral regulator of cancer metastasis via upregulation of pro-inflammatory cytokines release, cell survival, and immunosuppression.[12–14] Furthermore, STAT3 is found to be consistently activated in ovarian cancer cells that are exposed to ascites.[15,16] Western blot validation performed on CFA-treated Colo-205 and SNU-C1 cells showed activation of STAT3 signaling in PC was through phosphorylation at Tyr705 (Figures 1G and 1H). Interestingly, we did not find activation of JAK phosphorylation in the CFA-treated cells, suggesting that ascites activates STAT3 signaling in a non-canonical fashion (Figure S1).

Prospective single-centre clinical study validating a 3-biomarker prognostic panel in ascites

We next performed multi-omics analysis to identify putative STAT3 activators in ascites (Figure 2A). Firstly, proteomics analysis using the Harmonizome database identified 644 and 190 secreted proteins associated with ascites and peritoneal fluid, respectively. Of these, 58 proteins were shared between both types of fluid while 54 proteins were strongly enriched (top 10% by abundance), yielding 112 putative enriched proteins for downstream analysis. To identify STAT3-related genes, 1455 genes involved in STAT3 pathway are curated from KEGG database. Cross-referencing these genes with the NCBI BioSystem database identified 162 genes that produced secreted proteins. Combining both analyses, we identified 30 putative secreted paracrine factors in intra-abdominal fluid that were biologically active. Correlation with prognostic information from the TCGA and KM-plotter databases identified 14 putative secreted markers which were prognostic in at least three different cancer subtypes (Table S2).

To infer the biological and clinical significance of these selected secreted markers, we performed validation of five targets (PAI-1, MMP-9, IL-6, IL-10 and CCL-2) in an independent cohort of PC patients recruited prospectively in a single center (n = 149) (Table S3). Patients exhibiting high expression of individual biomarkers had poorer overall survival (OS) as compared to those with low expression, except for MMP-9 where no difference was observed (Figure S2). Examining the three most significant biomarkers (IL-6, PAI-1 and CCL-2) in combination showed

Figure 1. Ascites in peritoneal carcinomatosis (PC) is biologically active

(A) Kaplan-Meier curve showing survival of PC patients who underwent cytoreductive surgery (n = 121), stratified by the presence or absence of ascites.

(B and C) Proliferation curves of (B) Colo-205 and (C) SNU-C1 cells treated with varying concentrations of ascites, measured by CellTitre-Glo assay. Data are represented as cell viability at day 5 relative to day 0. Dotted line represents cell viability of Colo-205 treated with 10% fetal bovine serum (FBS) at day 5 relative to day 0. Graph shows mean ± SD.

(D and E) Migration of (D) Colo-205 and (E) SNU-C1 cells pre-treated with serum-free media (SFM), 10% FBS medium or 5% cell-free ascites (CFA) medium, assessed by transwell migration assay. Significant difference detected via unpaired two-sided t test between migration of cells pre-treated with SFM and 10% FBS or 5% CFA was denoted by *. *$p < 0.05$, **$p < 0.01$, ***$p < 0.001$. Significant difference detected via unpaired two-sided t test between migration of cells pre-treated with 10% FBS and SFM or 5% CFA was denoted by $^{\#}$. $^{\#}p < 0.05$, $^{\#\#}p < 0.01$, $^{\#\#\#}p < 0.001$. Graph shows mean ± SD.

(F) Enriched signaling pathways in colorectal PC cell lines upon treatment with CFA, identified by comparing gene expressions of cells treated with 5% versus 0.1% CFA. *$p < 0.05$, **$p < 0.01$, ***$p < 0.001$.

(G and H) Treatment of (G) Colo-205 and (H) SNU-C1 cells with 5% CFA activated STAT3 signaling pathway through phosphorylation at Tyr705.

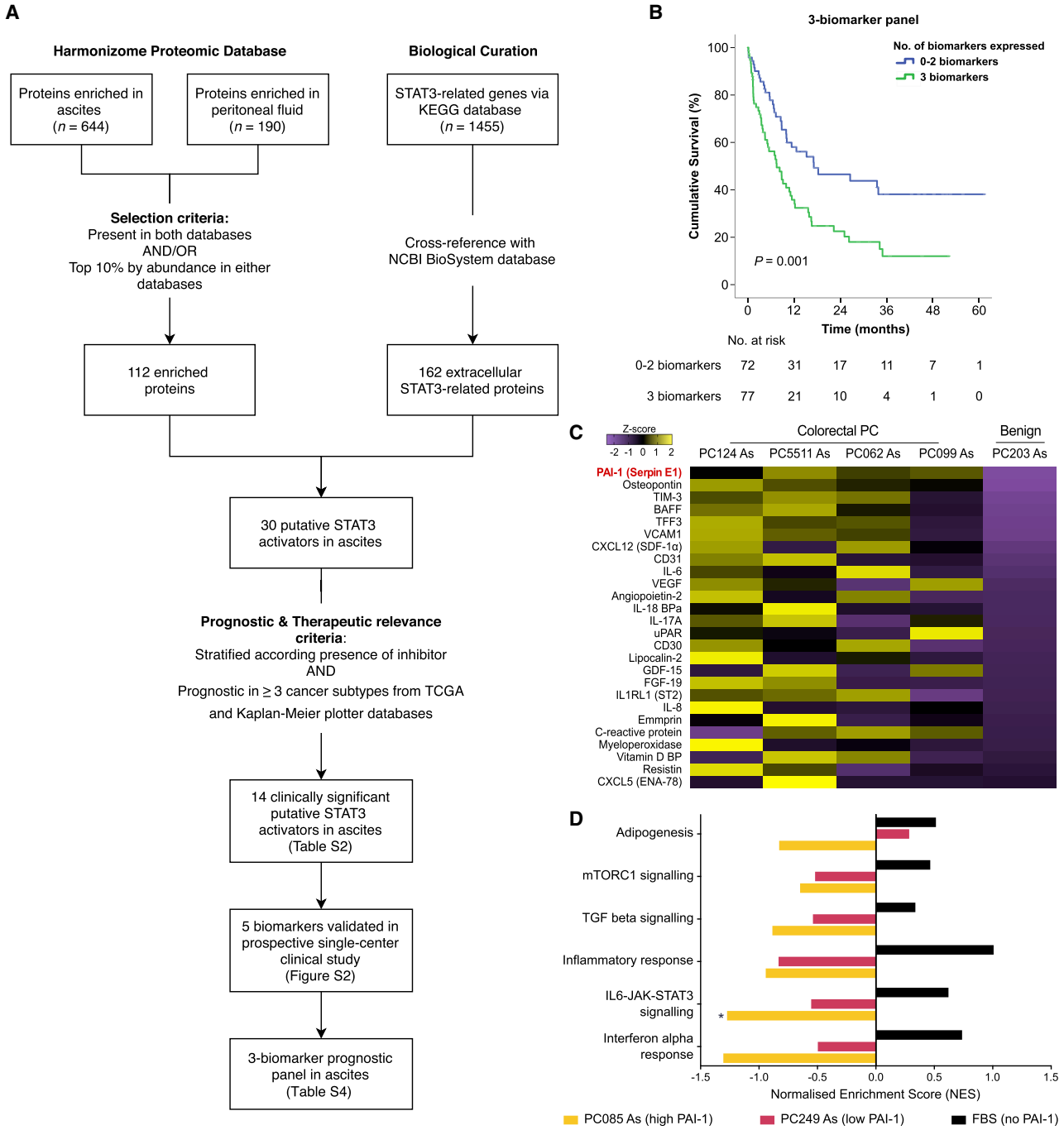

Figure 2. Identification and validation of prognostic putative activators of STAT3 signaling in ascites

(A) Workflow to identify clinically significant putative secreted STAT3 activators.

(B) Kaplan-Meier survival curve illustrating poorer survival in patients expressing three biomarkers as compared to patients expressing 0–2 biomarkers.

(C) Characterization of cytokine profiles in colorectal PC ascites and benign ascites. Top 25% most highly abundant cytokines in colorectal PC ascites (by mean abundance) are shown. Heatmap displays *Z* score of normalized mean pixel density of duplicate cytokine spots on the array.

(D) Downregulated signaling pathways upon PAI-1 inhibition in Colo-205 cells exposed to CFA with high PAI-1 levels (PC085), CFA with low PAI-1 levels (PC249) and no PAI-1 (FBS control), identified using RNA microarray. Only signaling pathways with differential downregulation are presented. IL6-JAK-STAT3 signaling pathway was significantly downregulated in high PAI-1 CFA-treated cells upon PAI-1 inhibition. Normalized enrichment scores <0 indicate pathway suppression and scores >0 indicate pathway activation. (D) is representative of two independent biological experiments. *$p < 0.05$.

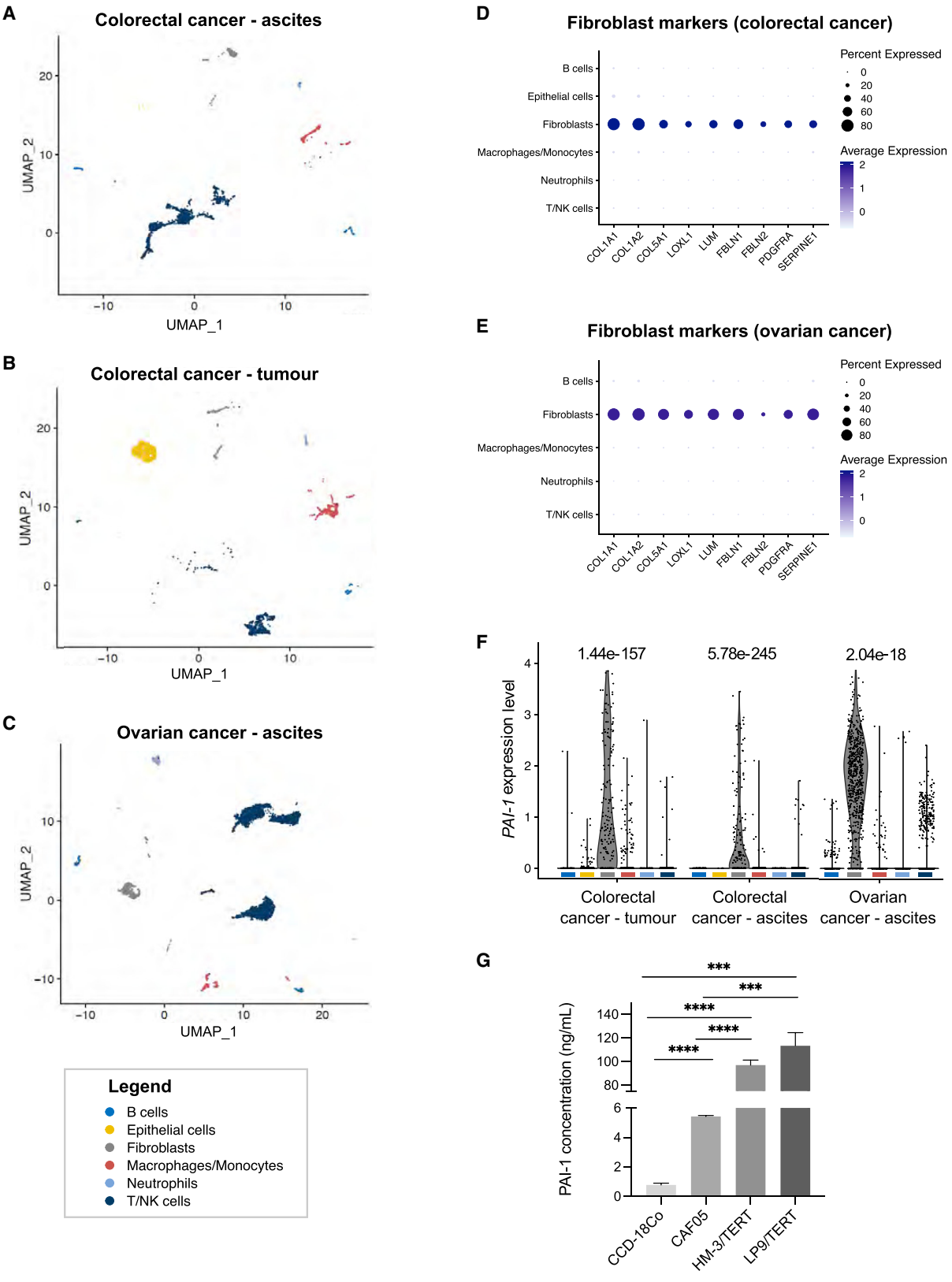

(legend on next page)

patients expressing three biomarkers with high expression had significantly poorer OS than patients expressing 0–2 biomarkers with high expression (p = 0.001) (Figure 2B). Multivariate analysis demonstrated that the 3-biomarker panel was independently prognostic of clinical covariates (p = 0.032) (Table S4).

PAI-1 in ascites is a putative activator of STAT3 signaling in PC cells

Consistently, when we compared the cytokine array profile of colorectal PC CFA (n = 4) to benign CFA (n = 1), we observed PAI-1 to be highly abundant in colorectal PC ascites, suggesting that PAI-1 could be a putative activator of STAT3 signaling (Figures 2C and S3). PAI-1 is a serine protease inhibitor with pleiotropic biological functions.[17] In the clinical setting, PAI-1 has been implicated in cardiovascular diseases, wound healing, metabolic diseases and cancer.[18] Despite its function as an inhibitor of tissue-type plasminogen activator, PAI-1 was found to be pro-angiogenic[19,20] and involved in tumor invasion.[21] A recent study has shown that PAI-1 promotes the recruitment and M2 polarization of macrophages via activation of p38 MAPK and NF-κB to induce an autocrine IL-6/STAT3 activation pathway.[22]

Measurement of PAI-1 level in 15 colorectal PC ascites revealed varying concentrations of PAI-1, which can be divided into two categories: high PAI-1 CFA and low PAI-1 CFA (Figure S4). To ascertain if PAI-1 mediates STAT3 activation in PC cells, we treated Colo-205 cells with high PAI-1 CFA, low PAI-1 CFA and FBS control (no PAI-1) in the presence of a PAI-1 inhibitor, TM5441. Pharmacological perturbation with PAI-1 inhibitor in Colo-205 cells exposed to high PAI-1 CFA revealed a significant downregulation in IL6-JAK-STAT3 pathway that was not observed in low PAI-1 or FBS groups (Normalized enrichment score (NES) = −1.27, p = 0.038) (Figure 2D). Taken together, these suggest that PAI-1 in ascites is a potential non-canonical activator of STAT3 signaling that is both prognostic and amenable to therapeutic perturbation via ligand inhibition.

Fibroblasts and mesothelial cells as key secretors of PAI-1 into ascites

PAI-1 is a well-recognized central regulator of fibrinolysis and coagulation.[23] To confirm that PAI-1 is a secreted factor and not a contaminant, we performed single-cell analysis to identify the specific cell types that expressed PAI-1. In colorectal cancer ascites obtained intraoperatively, we observed that the bulk of the cells were of immune origin, especially T/NK cells (71.5%). Epithelial cells, presumably tumour-derived, accounted for only 0.1% of the cell population (Figure 3A). On the other hand, colorectal tumor cells within matched peritoneal nodules from the same patient made up 31% of the total cell population (Figure 3B). This was similarly observed in the ovarian cancer ascites obtained intraoperatively (Figure 3C). *SERPINE1* (gene encoding PAI-1), along with other fibroblast-specific genes, were significantly expressed in fibroblasts but not in other cell types (Figures 3D and 3E). This was consistently observed in the colorectal (peritoneal tumor and ascites) and ovarian (ascites) cases (Figure 3F).

When we collected conditioned media from multiple cell line models 24 h after seeding, we observed that secreted PAI-1 levels from colorectal cancer cell lines representative of PC (SNU-C1 and Colo-205) measured via ELISA were below detection levels. Furthermore, normal mesothelial cells (HM-3/TERT and LP9/TERT) and colorectal tumor cancer-associated fibroblasts (CAF05) secreted significantly more PAI-1 into the conditioned media than normal colonic fibroblast (CCD-18Co) ($p < 0.001$) (Figure 3G). Taken together, the single-cell analysis along with the conditioned media experiment suggest that cancer cells exploit the paracrine activation of STAT3 signaling via secreted PAI-1 from fibroblasts and mesothelial cells.

Molecular stratification of ascites based on PAI-1 levels and downstream STAT3 activation

To robustly evaluate the biological impact of PAI-1 as a paracrine factor in the clinical setting via activation of STAT3 signaling, we systematically collected and processed 55 CFA isolated from colorectal PC patients. We then exposed Colo-205 cells to these CFA samples and measured the phosphorylation of STAT3 at residue Tyr705 to quantify the degree of STAT3 activation in cancer cells. We noted a trend toward higher STAT3 activation with increasing levels of PAI-1 ($r = 0.4691$, $p = 0.0003$) (Figures 4A and 4B).

To comprehensively evaluate the prevalence of this association in PC, we evaluated the PAI-1 levels in 156 samples of CFA from various histological PC subtypes (Table S5). PAI-1 concentrations were found to be highly variable across histological subtypes and were on average 1.3- to 5-fold (in $\log_2$ ratio) greater in malignant than in benign ascites samples (Figure 4C). Consistent with the observation in colorectal PC, PAI-1 levels were positively correlated with STAT3 activation ($r = 0.6476$, $p < 0.0001$) (Figure 4D). Similarly, PAI-1 levels and STAT3 activation were positively correlated in SNU-C1 cells treated with CFA from colorectal PC ($n = 35$, $r = 0.5510$, $p = 0.0006$) and various histological PC subtypes ($n = 77$, $r = 0.5239$, $p < 0.0001$) (Figures S5A and S5B). Furthermore, we noted that STAT3 activation in CFA-treated Colo-205 and SNU-C1 cells exhibited high positive

Figure 3. Single-cell analysis identifies tumour-associated fibroblasts as source expressing PAI-1

(A–C) UMAP plots showing composition of cell types in peritoneal tumors and ascites derived from colorectal and ovarian cancer.

(D and E) *SERPINE1* (gene encoding PAI-1), along with other fibroblast-specific genes, were significantly expressed in fibroblasts but not in other cell types for both the colorectal and ovarian cancer cases.

(F) Within the peritoneal nodules and ascites samples examined, *SERPINE1* is significantly expressed in fibroblasts over other cell types. Values represent p values adjusted for multiple hypotheses using the Bonferroni correction.

(G) PAI-1 secretion in stromal (mesothelial cells and fibroblasts) cell lines, measured in conditioned medium at 24 h by ELISA. CCD-18Co is a normal colonic fibroblast cell line, CAF05 is a colorectal tumor cancer-associated fibroblast cell line, and HM-3/TERT and LP9-TERT are normal peritoneal mesothelial cell lines. PAI-1 secretion in PC cell lines (SNU-C1 and Colo-205) were below the detection limit and not represented in the figure. (G) is representative of three independent biological experiments. Graph shows mean ± SEM. ***p < 0.001, ****p < 0.0001, unpaired two-sided t test.

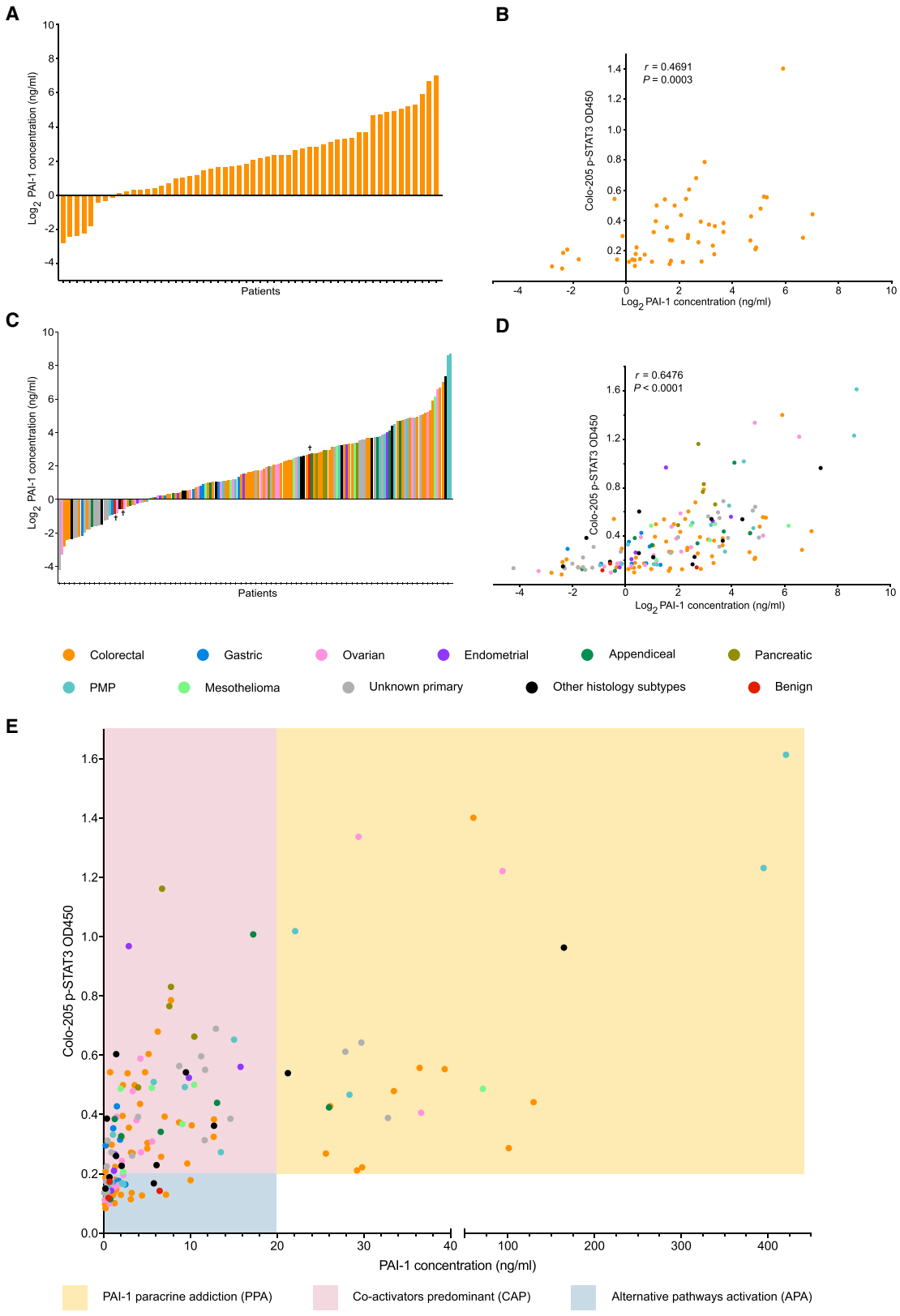

(legend continued on next page)

correlation ($r = 0.7353$, $p < 0.0001$), suggesting that the effects of ascites on pathway activation were largely dependent on ligand composition in the ascites as opposed to cell line specificity (Figure S5C).

We treated SNU-C1 cells with CFA to study the link between the untransformed (original values) PAI-1 levels in CFA with the corresponding degree of STAT3 phosphorylation in SNU-C1 cells exposed to these CFA (Figure S5D). Setting the phosphorylation of STAT3 (Tyr705) $\geq$ 0.2 (OD 450) as an arbitrary definition of activated STAT3 signaling, we noted that all samples with PAI-1 level above 20 ng/mL activated STAT3 signaling. Validation with another cell line model (Colo-205) was also performed. When the same threshold of phosphorylation of STAT3 (Tyr705) was applied, the observed stratification of samples were consistent (Figure 4E). Furthermore, the concordance rate of 99.91% between SNU-C1 and Colo-205 classification lends confidence to our molecular stratification model. This led us to propose three biological phenotypes of CFA. Firstly, CFA with PAI-1 levels $\geq$20 ng/mL relied heavily on PAI-1 to activate STAT3 signaling. We termed these samples PAI-1 paracrine addicted (PPA). Secondly, CFA with PAI-1 levels below 20 ng/mL but nevertheless activated STAT3 signaling in cells exposed to these CFA were termed co-activators predominant (CAP). In this group, STAT3 signaling was likely activated by a combination of PAI-1 and other ligands. Finally, CFA with PAI-1 below 20 ng/mL which failed to activate STAT3 signaling likely had ligands that activated other signaling pathways. We termed these samples alternative pathways activation (APA).

Here, we describe three subgroups of circulating tumor microenvironment with differing biological implications. Samples classified as PPA are uniquely dependent on PAI-1 within ascites for intracellular STAT3 activation. This dependence on PAI-1 is akin to the reliance of cancer cells on dominant driver oncogenes as described by the oncogene addiction theory.[24,25] Based on our findings, we postulate in a closed biological system characterized by a circulating microenvironment, cells can exhibit paracrine addiction hence providing an opportunity for therapeutic perturbation.

Exploiting paracrine addiction to PAI-1 for therapy

We next performed perturbation experiments by treating Colo-205 cell line with three subgroups of CFA and a PAI-1 inhibitor (TM5441) with the expectation that cells exposed to PPA ascites would be highly sensitive to PAI-1 inhibition. As predicted, cells exposed to PPA ascites were more susceptible to PAI-1 inhibition than CAP and APA ascites as determined by the PAI-1 and p-STAT3 stratification (Figures 5A and 5B). Treatment with a different PAI-1 inhibitor (Tiplaxtinin) had a similar, albeit weaker response than TM5441 (Figures S6A and S6B). Subsequently, we tested suppression of downstream signaling activated by PAI-1 using STAT3 inhibitor (Napabucasin) and observed lower efficacy in PPA group (Figures 5C and S6C). One possible explanation for this could be pleotropic roles of PAI-1 in promoting tumor progression, which resulted in concurrent activation of STAT3 and parallel intracellular signaling pathways, such as mTORC1, angiogenesis and EMT (as shown above) in response to PAI-1 stimulation. Inhibition of STAT3 alone would therefore have limited effects as alternative signaling pathways are able to partially compensate for this disruption. In addition, we tested chemotherapeutics targeting cancer cells proliferation (BEZ235 – dual PI3K/mTOR inhibitor) and DNA synthesis (Mitomycin C) and found that in all three subgroups of CFA, cancer cells exhibited resistance to the inhibitors (Figures 5D, 5E, S6D, and S6E). Altogether, our results demonstrate that ascites promotes chemoresistance in cancer cells and targeting key paracrine factor in ascites is a more efficacious therapeutic option than direct targeting of cancer cells.

To further demonstrate that reliance of cells treated with PPA ascites for STAT3 activation, we measured the levels of p-STAT3 in cells treated with PPA, CAP and APA ascites. Consistent with our hypothesis that PPA ascites is dependent on PAI-1 for STAT3 activation, we demonstrated that lower levels of TM5441 was needed to abrogate STAT3 activation in cells treated with PPA ascites compared to CAP and APA ascites (Figures 5F, S6F, and S6G).

In vivo validation and therapeutic efficacy of PAI-1 inhibition in PAI-1 paracrine addicted tumors

To recapitulate this phenomenon *in vivo*, we co-injected Colo-205 cells with CFA or FBS intraperitoneally in BALB/c nude mice to create a PC model and treated them with intraperitoneal (i.p.) injections of TM5441. Significantly lower tumor burden was observed in PPA ascites-treated mice but not others (PPA vs CAP, $p < 0.05$; PPA vs FBS, $p < 0.01$; CAP vs FBS, $p = 0.1392$)

Figure 4. Correlating PAI-1 level in ascites and intracellular STAT3 activation in cancer cells revealed distinct subgroups associated with differing susceptibility to PAI-1 inhibition

(A) PAI-1 prevalence in colorectal PC ascites (n = 54).

(B) Correlation between colorectal PC ascitic PAI-1 concentrations and ascites-treated Colo-205 cells p-STAT3(Y705) was determined by Pearson correlation coefficient test ($r = 0.4691$, $p = 0.0003$).

(C) PAI-1 prevalence in ascites of various histological PC subtypes (n = 156). † indicates benign ascites.

(D) Correlation between various histological PC ascitic PAI-1 concentrations and ascites-treated Colo-205 cells p-STAT3(Y705) was determined by Pearson correlation coefficient test ($r = 0.6476$, $p < 0.0001$).

(A–D) PAI-1 concentrations are plotted on a $\log_2$ scale to transform skewed data to normal distribution. p-STAT3(Y705) level was shown as optical density reading at 450 nm (OD450).

(E) Untransformed values of PAI-1 and p-STAT3(Y705) levels from (D) were used for stratification strategy to identify patient subpopulations who might benefit from PAI-1 inhibition. Using 20 ng/mL PAI-1 level and 0.2 OD450 p-STAT3(Y705) level as cut-off values, three distinct subgroups of samples were observed: (i) high PAI-1 and high p-STAT3 levels, termed PAI-1 paracrine addicted (PPA) group (yellow region), (ii) low PAI-1 and high p-STAT3 levels, termed co-activators predominant (CAP) group (pink region) and (iii) low PAI-1 and low p-STAT3 levels, termed alternative pathways activation (APA) group (blue region). Each dot represents one patient ascites. Colors in each panel represent the various histological PC subtypes. All histological subtypes with less than five samples are grouped into other histological subtypes.

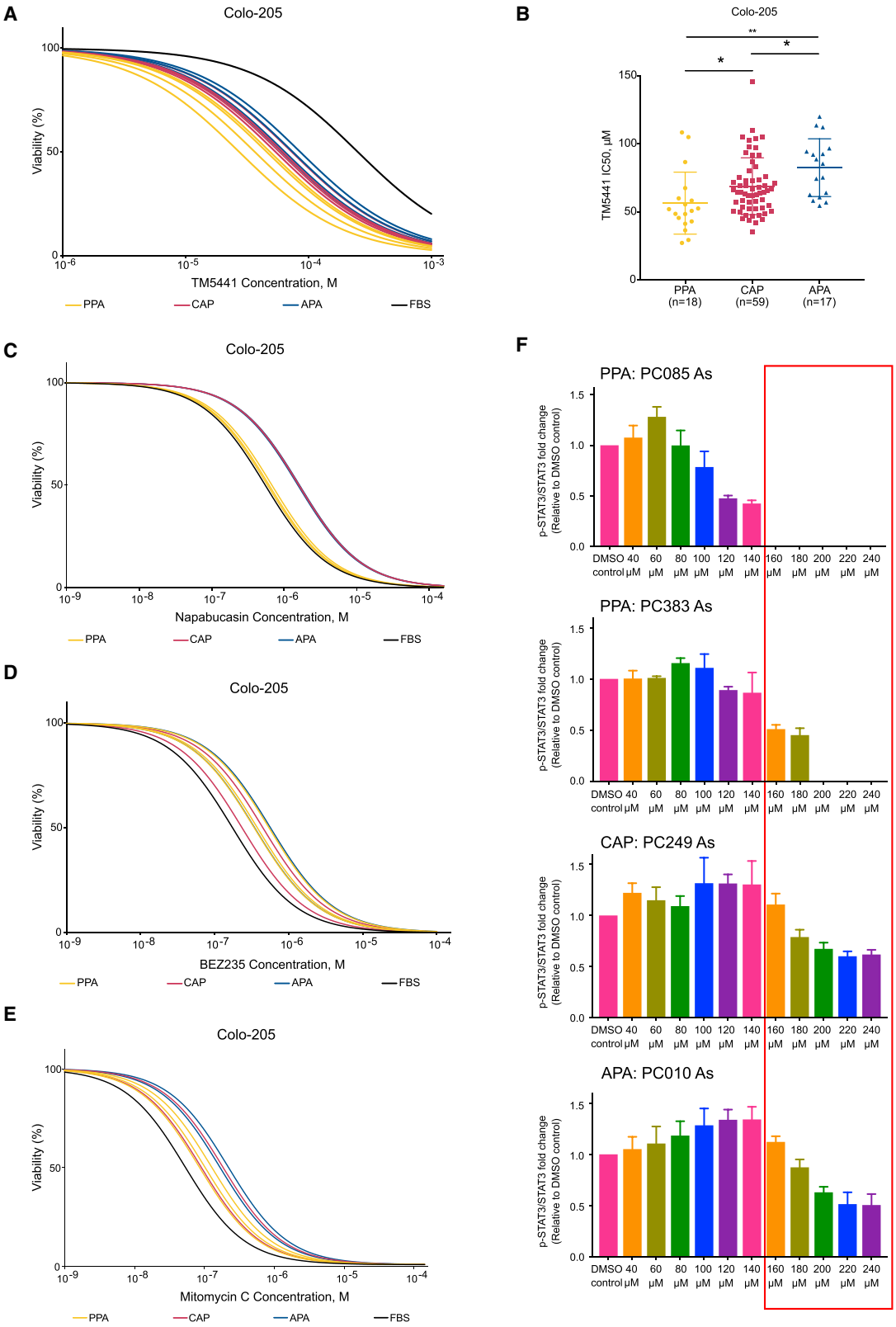

(legend on next page)

(Figures 6A and 6B). Furthermore, i.p. instillation of TM5441 greatly outperformed oral administration in the PC mouse model as shown by a lower tumor burden (2 mM TM5441 vs DMSO: i.p., $p < 0.0001$ and oral, $p = 0.287$) (Figures 6C and 6D). This is in line with the observation that in some histological subtypes of PC, systemic administration of drugs are relatively ineffective, with the exception of platinum-sensitive ovarian cancer.[26,27]

We next developed two patient-derived ascites-dependent xenografts (PDADXs), one from PPA group (PC383 PDADX) and one from CAP group (PC249 PDADX), to better recapitulate the PAI-1 addiction theory as a proxy of PC patients, taking into consideration both the tumors and paracrine-rich tumor microenvironment (Figure 6E). Genomic characterization of matched human peritoneal tumor, human ascites cells and PDADX tumors exhibited similar somatic mutations (Figure 6F). Additionally, morphological evaluation and immunohistochemical staining of the PDADX tumors confirmed that the tumors were of colonic origin (Figure 6G). When treated with TM5441, PC383 PDADX mice exposed to matched CFA from the same patient elicited a significantly superior inhibition of tumor growth compared to vehicle control and the FBS group ($p < 0.01$). In contrast, PC249 PDADX mice exposed to its matched patient's CFA and treated with TM5441 showed no difference in tumor burden compared to the vehicle control, ($p > 0.05$) (Figure 6H). Intriguingly, when PC249 PDADX mice were exposed to ascites from PPA group (PC383), these tumor cells became susceptible to PAI-1 inhibition, despite not being susceptible to PAI-1 inhibition in the presence of its own matched ascites (TM5441 vs DMSO: PC249 CFA, $p = 0.548$ and PC383 CFA, $p < 0.0001$) (Figure 6I). These results suggest that the paracrine microenvironment is capable of altering cancer cell phenotypes, independent of cancer cells' intrinsic signaling pathways/molecular aberrations, thus dictating the response to therapeutic ligand inhibition.

Taken together, we describe a phenomenon of paracrine addiction in the context of a closed biological niche where tumors along with their microenvironment are largely segregated from the systemic circulation. Paracrine factors in this context provide the key stimulus for pathway activation; paracrine inhibition provides the critical stop point (Figure 7). However, we also recognise the importance of the crosstalk between the biological niches of systemic and peritoneal compartments and more work will be necessary to elucidate it. This will provide a more comprehensive description of the biological niche within the peritoneal cavity.

DISCUSSION

Paget's "seed and soil" theory of cancer metastasis proposed more than a century ago provided the fundamentals of metastatic homing of tumor cells to distant sites.[28] Successful therapeutic strategies against the "seed" have focused on inhibiting cell division with chemotherapeutics[29–31] or exploiting molecular vulnerabilities of cancer cells oncogenically addicted to signaling pathways.[32–34] The advent of immunotherapy provided the second dimension of cancer treatment via altering the "soil" which cancer cells have rooted in.[35–38] To date, therapeutic strategies have not exploited the reliance of malignancies on paracrine factors; to target "water" to incite an arid desiccating environment untenable for tumor growth and survival. In this study, we describe an approach to identify prognostic biomarkers with therapeutic relevance, predict therapeutic response based on molecular stratification for patient selection, and demonstrate the efficacy of ligand inhibition through harnessing the concept of paracrine addiction.

Several studies have proposed multiple promising biomarkers to prognosticate PC patients, however, none have entered clinical practice.[39–42] Here, we utilize integrative analysis of publicly available proteomics and transcriptomic data to identify relevant putative STAT3 activators within ascites, and further prioritize them based on their clinical significance via correlation with prognostic information and therapeutic relevance in more than 7000 patients across multiple histological subtypes of cancers within the TCGA and Kaplan-Meier plotter databases. Validation of targets was performed in a prospective local cohort of PC patients which yielded a three-protein biomarker panel that was capable of prognosticating PC patients on multivariate analysis. In order to facilitate validation in larger cohort studies and future adaption into clinical practice, we have adhered closely to the REMARK guidelines[43] in the design of our study. Moving forward, we would also like to assess the use of this three-protein biomarker panel as a surrogate of STAT3 activation in PC cells and further refine the cut-off values for stratification to enable direct inference of molecular subgrouping and response to PAI-1 inhibition.

The role of PAI-1 as a critical regulator of peritoneal metastasis has been reported in ovarian and gastric PC.[44–46] However, unlike those studies, we found that PAI-1 is mainly secreted by stromal cells such as fibroblasts and mesothelial cells, and not cancer cells.[44] This suggests that the PAI-1 within ascites was

Figure 5. Cells dependent on PAI-1 to activate STAT3 are most susceptible to PAI-1 inhibition

(A) Effect of TM5441 (PAI-1 inhibitor) on CFA-treated Colo-205 cells. Representative inhibitor dose-response curves of PPA group (yellow), CAP group (pink), APA group (blue) and FBS (control, black) demonstrated a left shift, indicating responsiveness to PAI-1 inhibition.

(B) Differential sensitivity to TM5441 corresponding to the three subgroups, with PPA (n = 18) being the most sensitive to PAI-1 inhibition, followed by CAP (n = 59) and APA (n = 17). Graph shows mean ± SD.

(C–E) Effect of (C) Napabucasin (STAT3 inhibitor), (D) BEZ235 (dual PI3K/mTOR inhibitor) and (E) Mitomycin C (conventional chemotherapeutic agent – DNA crosslinker) on the three subgroups of ascites-treated Colo-205 cells. Representative inhibitor dose-response curves of PPA group (yellow; n = 3), CAP group (pink; n = 3), APA group (blue; n = 1) and FBS (control, black). Targeting PAI-1, a dominant paracrine factor in ascites, was more effective than targeting downstream signaling pathway activated by ascites, proliferation pathway or DNA synthesis.

(F) Evaluation of STAT3 suppression in Colo-205 cells treated with PPA CFA (PC085 and PC383), CAP CFA (PC249), APA CFA (PC010) and various concentrations of TM5441 by ELISA. STAT3 activation was shown as p-STAT3(Y705) and total STAT3 ratio at the indicated concentration relative to DMSO vehicle. Cells exposed to PPA CFA relied on PAI-1 to activate STAT3 as they required lower concentrations of TM5441 to suppress STAT3 activation. Graph shows mean ± SEM. Data in (A-E) are representative of at least three independent biological experiments and (F) is representative of two independent biological experiments. *$p < 0.05$, **$p < 0.01$.

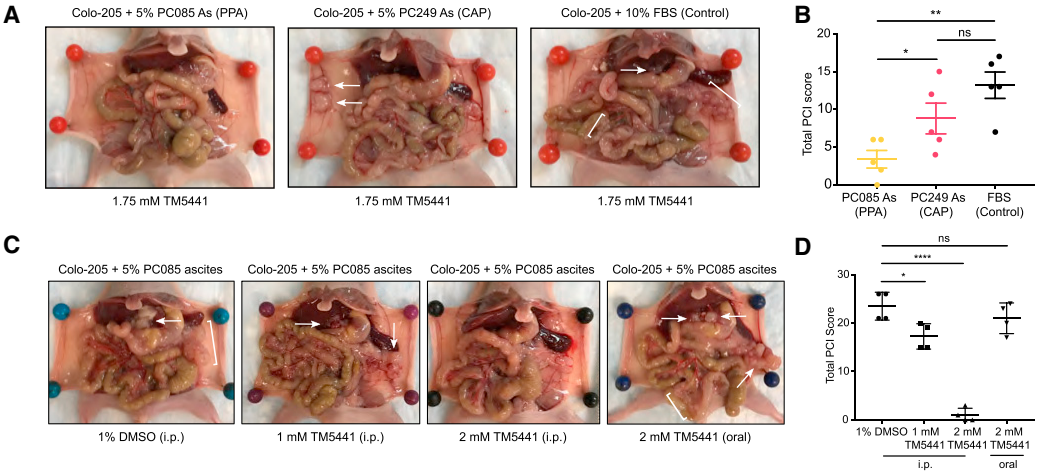

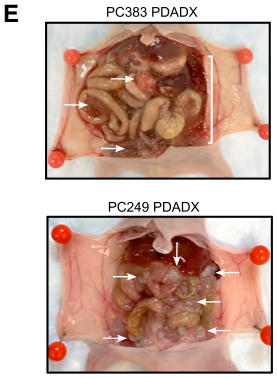

F

SN	Sample ID	NRAS Q61K	TP53 R150W
1	PC383 human peritoneal tumour	0.14	0.16
2	PC383 human ascites cell pellet	0.04	0.05
3	PC383 PDADX P1 Nude 1104 tumour	0.52	1.00
4	PC383 PDADX P1 Nude 1161 tumour	0.53	1.00

SN	Sample ID	APC E1518Q	APC E1536X	CHD1 K1337fs	KMT2D P2901fs
1	PC249 human peritoneal tumour	0.14	0.12	0.23	0.12
2	PC249 human ascites cell pellet	0.13	0.11	0.24	0.22
3	PC249 PDADX P1 Nude 1115 tumour	0.96	0.96	0.94	0.46
4	PC249 PDADX P2 Nude 1377 tumour	0.96	0.97	0.95	0.47

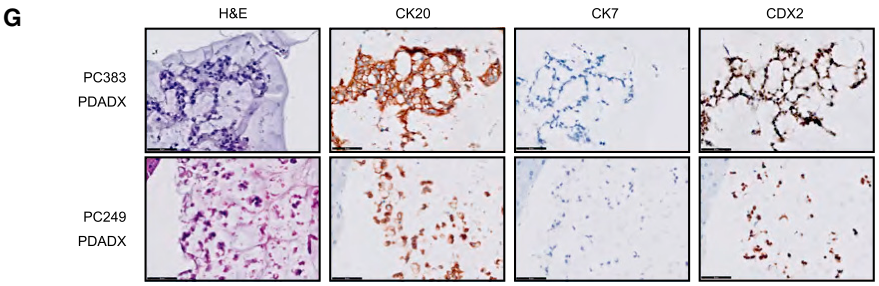

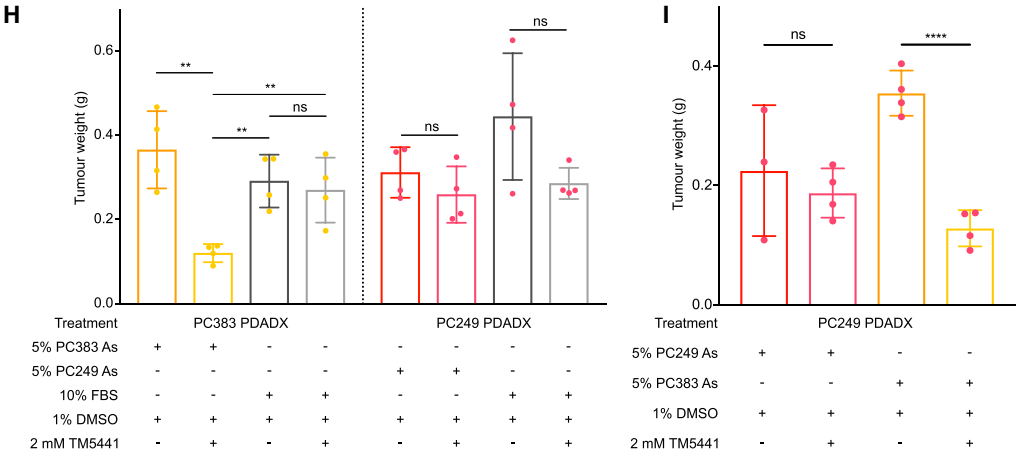

(legend on next page)

likely secreted by these cells and any biological effect of cancer cells via PAI-1 is paracrine in nature. Interestingly, in our single-cell analysis of PC cells in ascites, we noted high proportion of T/NK cells in the population (>70% in both colorectal and ovarian PC samples). This suggests that immunotherapy could potentially be a viable therapeutic strategy by utilizing PAI-1 antibody to promote antibody-dependent cellular cytotoxicity (ADCC) mediated by NK cells to kill PC cells.

Most importantly, our study also demonstrates that molecular stratification via evaluation of PAI-1 levels in ascites and downstream STAT3 activation in ascites-treated cells is key to successful prediction of therapeutic efficacy. Tumors reliant on PAI-1 for paracrine STAT3 activation is highly sensitive to PAI-1 inhibition and are able to overcome the chemoresistance conferred by the pro-tumorigenic effects of ascites. This highlights a key concept that successful therapy is possible in a subset of PC patients by exploiting the paracrine addiction phenomenon. From a clinical perspective, this concept is particularly attractive, as ascitic tap could be done to infer the molecular subgroup most likely to respond therapeutically. In addition, direct intraperitoneal instillation of ligand inhibition would present with lesser side effects compared to systemic administration since the peritoneal cavity is an enclosed biological space protected by the peritoneal-plasma barrier.

One limitation in our study is that we have not correlated the inherent genomic profile of peritoneal nodules, such as KRAS mutational or MSI status, with the molecular phenotype of ascites collected from these patients. Furthermore, while there are many drugs and antibodies targeting PAI-1,[47,48] there are currently no FDA approved drugs available.

mTORC1 signaling is another key signaling pathway upregulated in this study and is often found to be dysregulated in cancers. Multiple studies have also demonstrated the efficacy of mTOR inhibitors in halting cell cycle progression, cell death and angiogenesis.[49] Further investigations are therefore warranted to assess the potential utility of mTOR inhibition in PC. Moreover, future studies are essential to uncover other ligands and signaling pathways beyond PAI-1 and STAT3.

In conclusion, we have identified putative ligands that activate STAT3 signaling within ascites via a multi-omics discovery pipeline with subsequent independent prognostic validation in a prospective single-centre study. Harnessing the concept of paracrine addiction to a key biomarker within this panel for STAT3 activation, we demonstrate proof of concept of successful ligand inhibition *in vitro* and *in vivo* following molecular stratification of ascites. We do not profess that PAI-1 is the only dominant targetable paracrine factor in PC. On the contrary, it is our firm belief that the water holds many of the keys to successful therapeutics, be it in the form of signals for pathway activation or immunomodulatory mediators; all of which are prime targets for inhibition. Future studies shoud be performed to identify these ligands that may serve as alternative options for PC therapy.

Limitations of the study

Despite the elucidation that PAI-1 is predominantly secreted by mesothelial cells and fibroblasts, this study has not determined the co-factors that bind to PAI-1 in ascites to stimulate pro-tumorigenic reponse in cancer cells. This will be critical in the evaluation of opimal therapeutic candidates that will allow us to fully exploit the dependence of cancer cells on PAI-1 as the assay development typically involves direct perturbation of PAI-1 function biochemically and in *in vitro* studies using recombinant proteins to assess their biological effects. It is therefore important to perform further experiments to identify the co-factors needed to elucidate the homeostatic balance of proteins in the paracrine setting that will allow perturbation to take place. A potential strategy is to perform mass spectrometry analysis of ascites as a broad screening technique, coupled with a systematic pull-down experiment to identify potential binding partners of PAI-1, prior to the discovery of novel therapeutics for PAI-1.

Figure 6. PAI-1 inhibition is highly efficacious in PC cell line and PDADX mouse models that are addicted to PPA ascites

(A) Colo-205 cells were co-injected with CFA or FBS into the abdominal cavity of BALB/c nude mice and treated with 1.75 mM TM5441 by intraperitoneal (i.p.) injection. Ascites/FBS and drug treatment were repeated every 3 days for 21 days. Representative images of peritoneal metastases formed in response to treatment of ascites or FBS in the presence of PAI-1 inhibition. White arrows indicate visible tumors.

(B) Mice treated with PPA ascites (PC085) and TM5441 had significantly lower tumor burden compared to mice treated with CAP ascites (PC249) and FBS (n = 5 mice/group).

(C) Colo-205 cells were co-injected with 5% PPA CFA (PC085) into the abdominal cavity of BALB/c nude mice. DMSO vehicle or TM5441 (PAI-1 inhibitor) were administered intraperitoneally (i.p.) or orally (2 mM TM5441) every 3 days for a total of 21 days, to determine optimal drug concentration and drug delivery method (n = 4 mice/group). Representative images of peritoneal metastases formed in response to PAI-1 inhibition or vehicle DMSO. White arrows indicate visible tumors.

(D) Continuous i.p. administration of 2 mM TM5441 resulted in significantly lower tumor burden in PPA ascites-treated Colo-205 mouse model. Oral administration of inhibitor at the same concentration failed to lessen tumor formation. Tumor burdens in graphs (B) and (D) were assessed by modified peritoneal cancer index (PCI).

(E) Matched patient ascites and its cellular components were used to generate patient-derived ascites-dependent xenograft (PDADX). Representative images of intraperitoneal tumors formed in PC383 PDADX model (top) and PC249 PDADX model (bottom). White arrows indicate visible tumors.

(F) Whole exome sequencing of matched human peritoneal tumor, human ascites cells and PDADX tumors revealed consistent genetic features. Allele frequencies of key mutations found in PC383 whole exome sequencing (top) and PC249 whole exome sequencing (bottom).

(G) Representative haemotoxylin and Eosin (H&E) staining and immunohistochemical analyses confirmed PDADX tumors have similar histological features with their corresponding patient's tumor tissues and are of colonic origin (CK20 + CK7- CDX2+). Black scale bar, 50 μM.

(H) PPA PDADX (PC383) and CAP PDADX (PC249) were treated with its matched CFA or FBS in the presence of DMSO vehicle or 2 mM TM5441 (n = 4 mice/group). CFA/FBS and drug treatment was performed every 3 days for 21 days. Tumor burden was quantified by weighing all visible tumors after mice were sacrificed. Only PPA PDADX treated with matched PPA ascites was susceptible to PAI-1 inhibition and demonstrated significantly lower tumor burden.

(I) CAP PDADX (PC249) were treated with its matched ascites or PPA ascites (PC383) in the presence of DMSO vehicle or 2 mM TM5441 (n = 4 mice/group, except in group treated with PC249 ascites and DMSO, n = 3). CAP PDADX exposed to PPA ascites became susceptible to PAI-1 inhibition despite not being susceptible in the presence of its matched ascites. Graph in (B) shows mean ± SEM. Graphs in (D, H, and I) show mean ± SD. *$p < 0.05$, **$p < 0.01$, ****$p < 0.0001$, ns: not significant, unpaired two-sided t test.

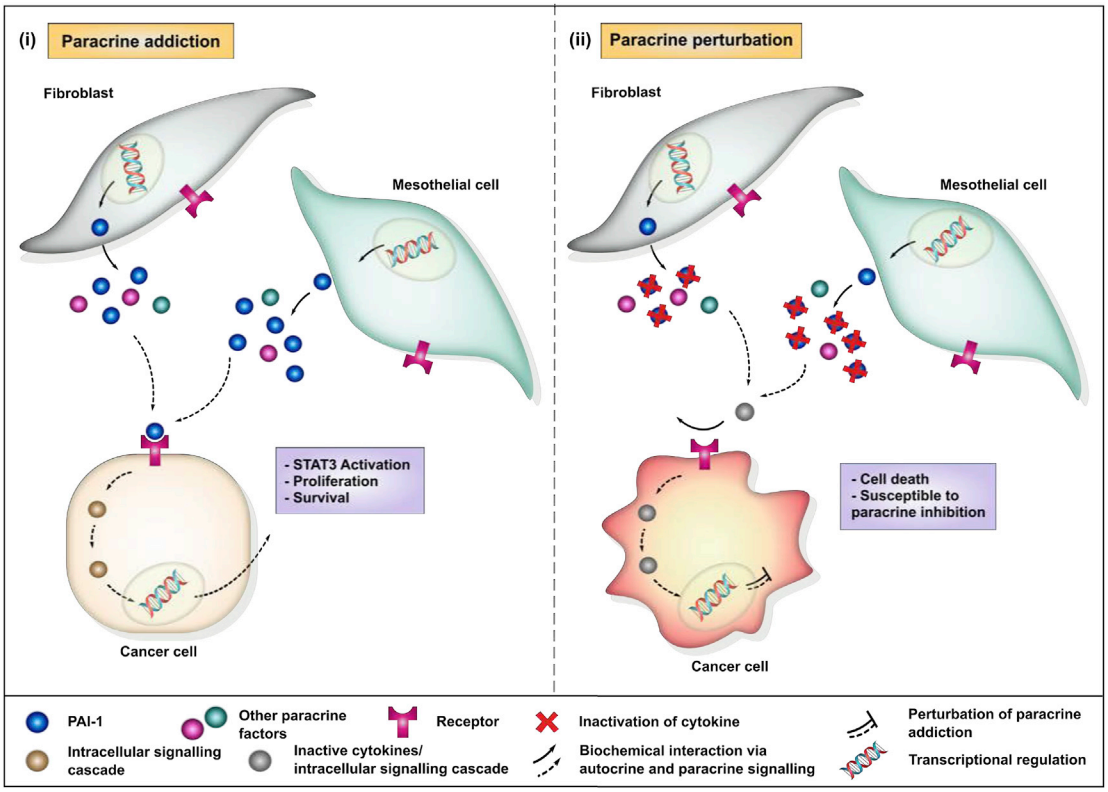

Figure 7. Proposed model of harnessing paracrine addiction for therapeutic perturbation

(i) Key paracrine factors in ascites activate intracellular signaling pathways within cancer cells to promote pro-tumorigenic responses. This leads to further secretion of these factors influencing both cancer cells and tumor microenvironment to facilitate tumor progression via autocrine and/or paracrine signaling. (ii) Upon perturbation of dominant paracrine factors, pro-tumorigenic signals and positive feedback loops are halted leading to cell death and improved therapeutic outcome.

Furthermore, the pleiotropic effect of PAI-1 is largely due to the active and latent forms of PAI-1 and the multiple sites of interaction with other proteins. Conceivably, side effects of PAI-1 inhibition, not limited to coagulation, may appear in the therapeutic setting and needs to be carefully monitored in a clinical trial.

STAR★METHODS

Detailed methods are provided in the online version of this paper and include the following:

- KEY RESOURCES TABLE
- RESOURCE AVAILABILITY
  - Lead contact
  - Materials availability
  - Data and code availability
- EXPERIMENTAL MODEL AND SUBJECT DETAILS
  - Patient recruitment and biospecimen collection
  - Cell lines
  - Animals
- METHOD DETAILS
  - Processing of patient derived specimens and fluids
  - Clinical data extraction
  - Proliferation assay
  - Cell migration assay
  - Integrative multi-omics analysis
  - Enzyme-linked immunosorbent assay (ELISA)
  - Validation of prognostic secreted biomarkers via ELISA
  - Single cell isolation, library preparation and sequencing
  - Analysis of single-cell sequencing data
  - Conditioned medium collection
  - RNA microarray and analysis
  - Whole exome sequencing and analysis
  - Human phospho-receptor tyrosine kinase (RTKs) profiling
  - Human cytokine profiling
  - Assessment of STAT3 activity in PC cells
  - Protein lysate preparation and western blot
  - Patient-derived ascites-dependent xenografts (PDADXs) generation
  - Immunohistochemical (IHC) staining
  - *In vivo* PC cell line mouse model drug treatment
  - PAI-1 inhibition of PDADX generated from matched ascites
  - PAI-1 inhibition of CAP PDADX in the presence of matched versus non-matched ascites

- QUANTIFICATION AND STATISTICAL ANALYSIS
  - Clinical endpoint and statistical analysis

SUPPLEMENTAL INFORMATION

Supplemental information can be found online at https://doi.org/10.1016/j.xcrm.2022.100526.

ACKNOWLEDGMENTS

The authors of this manuscript are part of the Singapore Gastric Cancer Consortium (SGCC). We would like to acknowledge S.T. Ong and X.Y.S. Ong from Duke-NUS Medical School, I.W.H. Tu and H.J. Lim from Ministry of Health Holdings, all members of the Singapore Peritoneal Oncology Study (SPOS) Group, and key members of the Asian Peritoneal Surface Malignancy Group (APSMG) for providing advice in the conduct of this study. This project is partially funded by the NCCS Cancer Fund (Research), NCC Research Fund as well as the SingHealth Duke-NUS Academic Medical Centre, facilitated by Joint Office of Academic Medicine (JOAM). As part of the Singapore Gastric Cancer Consortium, the study is also partially funded by the National Medical Research Council Open Fund-Large Collaborative Grant (OFLCG18May-0023). OCAJ is funded by the National Medical Research Council Transition Award (NMRC/TA/0061/2017). All the funding sources had no role in the study design, data interpretation or writing of the manuscript.

AUTHOR CONTRIBUTIONS

Conceptualization: C.-A.J.O.; data curation: J.H., W.H.N., Y.L., J.W.S.T., Q.X.T., and G.N.; formal analysis: J.H., W.H.N., Y.L., J.Y.L., A.H.L., J.W.L., C.C.Y.N., W.S.O., J.W.S.T., Q.X.T., G.N., N.B.S., W.K.L., and T.K.H.L.; funding acquisition: C.-A.J.O.; investigation: J.H., W.H.N., Y.L., J.Y.L., A.H.L., J.W.L., C.C.Y.N., J.W.S.T., Q.X.T., G.N., N.B.S., W.K.L., and T.K.H.L.; methodology: J.H. and C.-A.J.O.; project administration: J.H., Q.X.T., and C.-A.J.O.; resources: G.H.C.T., B.T.T., C.S.C., K.C.S., O.L.K., J.Y.C., M.C.C.T., and C.-A.J.O.; supervision: C.C., J.S.M.W., G.H.C.T., J.B.Y.S., K.G.Y., B.T.T., C.S.C., K.C.S., O.L.K., I.B.T., J.Y.C., M.C.C.T., and C.-A.J.O.; validation: J.H., W.H.N., Y.L., J.Y.L., A.H.L., J.W.L., C.C.Y.N., J.W.S.T., Q.X.T., G.N., N.B.S., W.K.L., and T.K.H.L.; visualization: J.H., Q.X.T., and J.W.S.T.; writing – original draft: J.H. and C.-A.J.O.; writing – review and editing: J.H., W.H.N., Y.L., J.Y.L., A.H.L., J.W.L., C.C.Y.N., W.S.O., J.W.S.T., Q.X.T., G.N., N.B.S., W.K.L., T.K.H.L., C.C., J.S.M.W., G.H.C.T., J.B.Y.S., K.G.Y., B.T.T., C.S.C., K.C.S., O.L.K., I.B.T., J.Y.C., M.C.C.T., and C.-A.J.O.

DECLARATION OF INTERESTS

C.-A.J.O., J.H., Y.L., W.H.N., J.W.S.T., Q.X.T., G.H.C.T., C.S.C., and M.C.C.T. report a Patent Cooperation Treaty (PCT) filed by Singapore Health Services for PAI-1 as a biomarker with therapeutic implications for peritoneal carcinomatosis (PCT/SG2020/050177). All of the other authors declare no competing interests.

Received: August 1, 2021
Revised: November 22, 2021
Accepted: January 19, 2022
Published: February 15, 2022

REFERENCES

1. Coccolini, F., Gheza, F., Lotti, M., Virzì, S., Iusco, D., Ghermandi, C., Melotti, R., Baiocchi, G., Giulini, S.M., Ansaloni, L., and Catena, F. (2013). Peritoneal carcinomatosis. World J. Gastroenterol. *19*, 6979.
2. Lane, D., Matte, I., Rancourt, C., and Piché, A. (2011). Prognostic significance of IL-6 and IL-8 ascites levels in ovarian cancer patients. BMC Cancer *11*, 210.
3. Matte, I., Lane, D., Laplante, C., Rancourt, C., and Piché, A. (2012). Profiling of cytokines in human epithelial ovarian cancer ascites. Am. J. Cancer Res. *2*, 566–580.
4. Zhan, N., Dong, W.G., and Wang, J. (2016). The clinical significance of vascular endothelial growth factor in malignant ascites. Tumour Biol. *37*, 3719–3725.
5. Fushida, S., Oyama, K., Kinoshita, J., Yagi, Y., Okamoto, K., Tajima, H., Ninomiya, I., Fujimura, T., and Ohta, T. (2013). VEGF is a target molecule for peritoneal metastasis and malignant ascites in gastric cancer: prognostic significance of VEGF in ascites and efficacy of anti-VEGF monoclonal antibody. Onco Targets Ther. *6*, 1445.
6. Jin, J., Son, M., Kim, H., Kim, H., Kong, S.H., Kim, H.K., Kim, Y., and Han, D. (2018). Comparative proteomic analysis of human malignant ascitic fluids for the development of gastric cancer biomarkers. Clin. Biochem. *56*, 55–61.
7. Mesiano, S., Ferrara, N., and Jaffe, R.B. (1998). Role of vascular endothelial growth factor in ovarian cancer: inhibition of ascites formation by immunoneutralization. Am. J. Pathol. *153*, 1249–1256.
8. Herr, D., Sallmann, A., Bekes, I., Konrad, R., Holzheu, I., Kreienberg, R., and Wulff, C. (2012). VEGF induces ascites in ovarian cancer patients via increasing peritoneal permeability by downregulation of Claudin 5. Gynecol. Oncol. *127*, 210–216.
9. Ford, C.E., Werner, B., Hacker, N.F., and Warton, K. (2020). The untapped potential of ascites in ovarian cancer research and treatment. Br. J. Cancer *123*, 9–16.
10. Amini, A., Masoumi Moghaddam, S., Morris, D.L., and Pourgholami, M.H. (2012). Utility of vascular endothelial growth factor inhibitors in the treatment of ovarian cancer: from concept to application. J. Oncol. *2012*, 1–14.
11. Parsons, S.L., Lang, M.W., and Steele, R.J. (1996). Malignant ascites: a 2-year review from a teaching hospital. Eur. J. Surg. Oncol. *22*, 237–239.
12. Bournazou, E., and Bromberg, J. (2013). Targeting the tumor microenvironment: JAK-STAT3 signaling. JAKSTAT *2*, e23828.
13. Lee, H., Jeong, A.J., and Ye, S.K. (2019). Highlighted STAT3 as a potential drug target for cancer therapy. BMB Rep. *52*, 415–423.
14. Huynh, J., Chand, A., Gough, D., and Ernst, M. (2019). Therapeutically exploiting STAT3 activity in cancer - using tissue repair as a road map. Nat. Rev. Cancer *19*, 82–96.
15. Saini, U., Naidu, S., ElNaggar, A.C., Bid, H.K., Wallbillich, J.J., Bixel, K., Bolyard, C., Suarez, A.A., Kaur, B., Kuppusamy, P., et al. (2017). Elevated STAT3 expression in ovarian cancer ascites promotes invasion and metastasis: a potential therapeutic target. Oncogene *36*, 168–181.
16. Jiang, Y.X., Siu, M.K., Wang, J.J., Mo, X.T., Leung, T.H., Chan, D.W., Cheung, A.N., Ngan, H.Y., and Chan, K.K. (2020). Ascites-derived ALDH+CD44+ tumour cell subsets endow stemness, metastasis and metabolic switch via PDK4-mediated STAT3/AKT/NF-κB/IL-8 signalling in ovarian cancer. Br. J. Cancer *123*, 275–287.
17. Cesari, M., Pahor, M., and Incalzi, R.A. (2010). Plasminogen activator inhibitor-1 (PAI-1): a key factor linking fibrinolysis and age-related subclinical and clinical conditions. Cardiovasc. Ther. *28*, e72–e91.
18. Placencio, V.R., and DeClerck, Y.A. (2015). Plasminogen activator inhibitor-1 in cancer: rationale and insight for future therapeutic testing. Cancer Res. *75*, 2969–2974.
19. Bajou, K., Masson, V., Gerard, R.D., Schmitt, P.M., Albert, V., Praus, M., Lund, L.R., Frandsen, T.L., Brunner, N., Dano, K., et al. (2001). The plasminogen activator inhibitor PAI-1 controls in vivo tumor vascularization by interaction with proteases, not vitronectin. Implications for antiangiogenic strategies. J. Cell Biol. *152*, 8.
20. Isogai, C., Laug, W.E., Shimada, H., Declerck, P.J., Stins, M.F., Durden, D.L., Erdreich-Epstein, A., and DeClerck, Y.A. (2001). Plasminogen activator inhibitor-1 promotes angiogenesis by stimulating endothelial cell migration toward fibronectin. Cancer Res. *61*, 5587–5594.
21. Freytag, J., Wilkins-Port, C.E., Higgins, C.E., Carlson, J.A., Noel, A., Foidart, J.M., Higgins, S.P., Samarakoon, R., and Higgins, P.J. (2009). PAI-

1 regulates the invasive phenotype in human cutaneous squamous cell carcinoma. J. Oncol. *2009*, 1–12.

22. Kubala, M.H., Punj, V., Placencio-Hickok, V.R., Fang, H., Fernandez, G.E., Sposto, R., and DeClerck, Y.A. (2018). Plasminogen activator inhibitor-1 promotes the recruitment and polarization of macrophages in cancer. Cell Rep. *25*, 2177–2191.
23. Hermans, P.W., and Hazelzet, J.A. (2005). Plasminogen activator inhibitor type 1 gene polymorphism and sepsis. Clin. Infect. Dis. *41*, S453–S458.
24. Weinstein, I.B. (2000). Disorders in cell circuitry during multistage carcinogenesis: the role of homeostasis. Carcinogenesis *21*, 857–864.
25. Weinstein, I.B. (2002). Cancer. Addiction to oncogenes–the Achilles heal of cancer. Science *297*, 63–64.
26. Sadeghi, B., Arvieux, C., Glehen, O., Beaujard, A.C., Rivoire, M., Baulieux, J., Fontaumard, E., Brachet, A., Caillot, J.L., Faure, J.L., et al. (2000). Peritoneal carcinomatosis from non-gynecologic malignancies: results of the EVOCAPE 1 multicentric prospective study. Cancer *88*, 358–363.
27. Tomao, F., D'Incalci, M., Biagioli, E., Peccatori, F.A., and Colombo, N. (2017). Restoring platinum sensitivity in recurrent ovarian cancer by extending the platinum-free interval: myth or reality? Cancer *123*, 3450–3459.
28. Paget, S. (1889). The distribution of secondary growths in cancer of the breast. Lancet *133*, 571–573.
29. Farber, S., Diamond, L.K., Mercer, R.D., Sylvester, R.F., and Wolff, J.A. (1948). Temporary remissions in acute leukemia in children produced by folic acid antagonist, 4-aminopteroyl-glutamic acid. N. Engl. J. Med. *238*, 787–793.
30. Devita, V.T., Serpick, A.A., and Carbone, P.P. (1970). Combination chemotherapy in the treatment of advanced Hodgkin's disease. Ann. Intern. Med. *73*, 881–895.
31. Einhorn, L.H., and Donohue, J. (1977). Cis-Diamminedichloroplatinum, Vinblastine, and Bleomycin combination chemotherapy in disseminated testicular cancer. Ann. Intern. Med. *87*, 293–298.
32. Slamon, D.J., Leyland-Jones, B., Shak, S., Fuchs, H., Paton, V., Bajamonde, A., Fleming, T., Eiermann, W., Wolter, J., Pegram, M., et al. (2001). Use of chemotherapy plus a monoclonal antibody against HER2 for metastatic breast cancer that overexpresses HER2. N. Engl. J. Med. *344*, 783–792.
33. Druker, B.J., Tamura, S., Buchdunger, E., Ohno, S., Segal, G.M., Fanning, S., Zimmermann, J., and Lydon, N.B. (1996). Effects of a selective inhibitor of the Abl tyrosine kinase on the growth of Bcr-Abl positive cells. Nat. Med. *2*, 561–566.
34. Demetri, G.D., von Mehren, M., Blanke, C.D., Van den Abbeele, A.D., Eisenberg, B., Roberts, P.J., Heinrich, M.C., Tuveson, D.A., Singer, S., Janicek, M., et al. (2002). Efficacy and safety of Imatinib mesylate in advanced gastrointestinal stromal tumors. N. Engl. J. Med. *347*, 472–480.
35. Hodi, F.S., Mihm, M.C., Soiffer, R.J., Haluska, F.G., Butler, M., Seiden, M.V., Davis, T., Henry-Spires, R., MacRae, S., Willman, A., et al. (2003). Biologic activity of cytotoxic T lymphocyte-associated antigen 4 antibody blockade in previously vaccinated metastatic melanoma and ovarian carcinoma patients. Proc. Natl. Acad. Sci. U S A *100*, 4712–4717.
36. Hodi, F.S., O'Day, S.J., McDermott, D.F., Weber, R.W., Sosman, J.A., Haanen, J.B., Gonzalez, R., Robert, C., Schadendorf, D., Hassel, J.C., et al. (2010). Improved survival with Ipilimumab in patients with metastatic melanoma. N. Engl. J. Med. *363*, 711–723.
37. Pardoll, D.M. (2012). The blockade of immune checkpoints in cancer immunotherapy. Nat. Rev. Cancer *12*, 252–264.
38. Kalos, M., Levine, B.L., Porter, D.L., Katz, S., Grupp, S.A., Bagg, A., and June, C.H. (2011). T cells with chimeric antigen receptors have potent antitumor effects and can establish memory in patients with advanced leukemia. Sci. Transl. Med. *3*, 95ra73.
39. Kern, S.E. (2012). Why your new cancer biomarker may never work: recurrent patterns and remarkable diversity in biomarker failures. Cancer Res. *72*, 6097–6101.
40. Koumpa, F.S., Xylas, D., Konopka, M., Galea, D., Veselkov, K., Antoniou, A., Mehta, A., and Mirnezami, R. (2019). Colorectal peritoneal metastases: a systematic review of current and emerging trends in clinical and translational research. Gastroenterol. Res. Pract. *2019*, 1.
41. Chen, Y., Zhou, Q., Wang, H., Zhuo, W., Ding, Y., Lu, J., Wu, G., Xu, N., and Teng, L. (2020). Predicting peritoneal dissemination of gastric cancer in the era of precision medicine: molecular characterization and biomarkers. Cancers (Basel) *12*, E2236.
42. Alain, P. (2018). IL-6 and VEGF-A, novel prognostic biomarkers for ovarian cancer? J. Lab. Precis. Med. *3*, 48.
43. McShane, L.M., Altman, D.G., Sauerbrei, W., Taube, S.E., Gion, M., and Clark, G.M. (2005). REporting recommendations for tumour MARKer prognostic studies (REMARK). Br. J. Cancer *93*, 387–391.
44. Peng, Y., Kajiyama, H., Yuan, H., Nakamura, K., Yoshihara, M., Yokoi, A., Fujikake, K., Yasui, H., Yoshikawa, N., Suzuki, S., et al. (2019). PAI-1 secreted from metastatic ovarian cancer cells triggers the tumor-promoting role of the mesothelium in a feedback loop to accelerate peritoneal dissemination. Cancer Lett. *442*, 181–192.
45. Nakatsuka, E., Sawada, K., Nakamura, K., Yoshimura, A., Kinose, Y., Kodama, M., Hashimoto, K., Mabuchi, S., Makino, H., Morii, E., et al. (2017). Plasminogen activator inhibitor-1 is an independent prognostic factor of ovarian cancer and IMD-4482, a novel plasminogen activator inhibitor-1 inhibitor, inhibits ovarian cancer peritoneal dissemination. Oncotarget *8*, 89887–89902.
46. Nishioka, N., Matsuoka, T., Yashiro, M., Hirakawa, K., Olden, K., and Roberts, J.D. (2012). Plasminogen activator inhibitor 1 RNAi suppresses gastric cancer metastasis in vivo. Cancer Sci. *103*, 228–232.
47. Rouch, A., Vanucci-Bacqué, C., Bedos-Belval, F., and Baltas, M. (2015). Small molecules inhibitors of plasminogen activator inhibitor-1 - an overview. Eur. J. Med. Chem. *92*, 619–636.
48. Sillen, M., and Declerck, P.J. (2020). Targeting PAI-1 in cardiovascular disease: structural insights into PAI-1 functionality and inhibition. Front .Cardiovasc. Med. *7*, 622473.
49. Faivre, S., Kroemer, G., and Raymond, E. (2006). Current development of mTOR inhibitors as anticancer agents. Nat. Rev. Drug Discov. *5*, 671–688.
50. Rouillard, A.D., Gundersen, G.W., Fernandez, N.F., Wang, Z., Monteiro, C.D., McDermott, M.G., and Ma'ayan, A. (2016). The harmonizome: a collection of processed datasets gathered to serve and mine knowledge about genes and proteins. Database (Oxford) *2016*, baw100.
51. Kanehisa, M., and Goto, S. (2000). KEGG: kyoto encyclopedia of genes and genomes. Nucleic Acids Res. *28*, 27–30.
52. Geer, L.Y., Marchler-Bauer, A., Geer, R.C., Han, L., He, J., He, S., Liu, C., Shi, W., and Bryant, S.H. (2010). The NCBI BioSystems database. Nucleic Acids Res. *38*, D492–D496.
53. National Cancer Institute. The cancer genome Atlas program [internet].https://www.cancer.gov/tcga.
54. Zheng, G.X.Y., et al. (2017). Massively parallel digital transcriptional profiling of single cells. Nature Communications *8*, 14049. https://doi.org/10.1038/ncomms14049.
55. Stuart, T., Butler, A., Hoffman, P., Hafemeister, C., Papalexi, E., Mauck, W.M., Hao, Y., Stoeckius, M., Smibert, P., and Satija, R. (2019). Comprehensive integration of single-cell data. Cell *177*, 1888–1902.e21.
56. Aran, D., Looney, A.P., Liu, L., Wu, E., Fong, V., Hsu, A., Chak, S., Naikawadi, R.P., Wolters, P.J., Abate, A.R., et al. (2019). Reference-based analysis of lung single-cell sequencing reveals a transitional profibrotic macrophage. Nat. Immunol. *20*, 163–172.
57. Carvalho, B. pd.hugene.2.0.st: platform design Info for Affymetrix HuGene-2_0-st. R package version 3.14.1. 2015.
58. Li, H., and Durbin, R. (2009). Fast and accurate short read alignment with Burrows-Wheeler transform. Bioinformatics *25*, 1754–1760.
59. Faust, G.G., and Hall, I.M. (2014). SAMBLASTER: fast duplicate marking and structural variant read extraction. Bioinformatics *30*, 2503–2505.

60. Tarasov, A., Vilella, A.J., Cuppen, E., Nijman, I.J., and Prins, P. (2015). Sambamba: fast processing of NGS alignment formats. Bioinformatics *31*, 2032–2034.

61. Conway, T., Wazny, J., Bromage, A., Tymms, M., Sooraj, D., Williams, E.D., and Beresford-Smith, B. (2012). Xenome–a tool for classifying reads from xenograft samples. Bioinformatics *28*, i172–i178.

62. Wang, K., Li, M., and Hakonarson, H. (2010). ANNOVAR: functional annotation of genetic variants from high-throughput sequencing data. Nucleic Acids Res. *38*, e164.

63. Amin, M.B., Greene, F.L., Edge, S.B., Compton, C.C., Gershenwald, J.E., Brookland, R.K., Meyer, L., Gress, D.M., Byrd, D.R., and Winchester, D.P. (2017). The eighth edition AJCC cancer staging manual: continuing to build a bridge from a population-based to a more "personalized" approach to cancer staging. CA Cancer J. Clin. *67*, 93–99.

64. Berek, J.S., Kehoe, S.T., Kumar, L., and Friedlander, M. (2018). Cancer of the ovary, fallopian tube, and peritoneum. Int. J. Gynaecol. Obstet. *143*, 59–78.

65. Sugarbaker, P.H. (1998). Intraperitoneal chemotherapy and cytoreductive surgery for the prevention and treatment of peritoneal carcinomatosis and sarcomatosis. Semin. Surg. Oncol. *14*, 254–261.

66. Nagy, Á., Munkácsy, G., and Győrffy, B. (2021). Pancancer survival analysis of cancer hallmark genes. Sci. Rep. *11*, 6047.

67. Peters, C.J., Rees, J.R., Hardwick, R.H., Hardwick, J.S., Vowler, S.L., Ong, C.A., Zhang, C., Save, V., O'Donovan, M., Rassl, D., et al. (2010). A 4-gene signature predicts survival of patients with resected adenocarcinoma of the esophagus, junction, and gastric cardia. Gastroenterology *139*, 1995–2004.

68. Ong, C.A., Shapiro, J., Nason, K.S., Davison, J.M., Liu, X., Ross-Innes, C., O'Donovan, M., Dinjens, W.N., Biermann, K., Shannon, N., et al. (2013). Three-gene immunohistochemical panel adds to clinical staging algorithms to predict prognosis for patients with esophageal adenocarcinoma. J. Clin. Oncol. *31*, 1576–1582.

69. Ong, C.-A.J., Shannon, N.B., Ross-Innes, C.S., O'Donovan, M., Rueda, O.M., Hu, D.-E., Kettunen, M.I., Walker, C.E., Noorani, A., Hardwick, R.H., et al. (2014). Amplification of TRIM44: pairing a prognostic target with potential therapeutic strategy. J. Natl. Cancer Inst. *106*. https://academic.oup.com/jnci/article-lookup/doi/10.1093/jnci/dju050.

70. Ong, C.J., Shannon, N.B., Mueller, S., Lek, S.M., Qiu, X., Chong, F.T., Li, K., Koh, K.K.N., Tay, G.C.A., Skanthakumar, T., et al. (2017). A three gene immunohistochemical panel serves as an adjunct to clinical staging of patients with head and neck cancer. Oncotarget *8*, 79556–79566.

71. Tarashansky, A.J., Xue, Y., Li, P., Quake, S.R., and Wang, B. (2019). Self-assembling manifolds in single-cell RNA sequencing data. eLife *8*, e48994.

72. Subramanian, A., Tamayo, P., Mootha, V.K., Mukherjee, S., Ebert, B.L., Gillette, M.A., Paulovich, A., Pomeroy, S.L., Golub, T.R., Lander, E.S., and Mesirov, J.P. (2005). Gene set enrichment analysis: a knowledge-based approach for interpreting genome-wide expression profiles. Proc. Natl. Acad. Sci. U S A *102*, 15545–15550.

73. R Core Team. R (2021). A Launguage and Environment for Statistical Computing (R Foundation for Statistical Computing). https://www.R-project.org/.

STAR★METHODS

KEY RESOURCES TABLE

REAGENT or RESOURCE	SOURCE	IDENTIFIER
Antibodies		
total STAT3	Cell Signalling Technology	4904, RRID: AB_331269
p-STAT3 (Ser727)	Cell Signalling Technology	94994, RRID: AB_2800239
p-STAT3 (Tyr705)	Cell Signalling Technology	9145, RRID: AB_2491009
JAK1	Santa Cruz Biotechnology	sc-277, RRID: AB_631851
p-JAK1 (Tyr1022/Tyr1023)	Santa Cruz Biotechnology	sc-16773, AB_653285
JAK2	Santa Cruz Biotechnology	sc-294, RRID: AB_631854
p-JAK2 (Tyr1007/Tyr1008)	Santa Cruz Biotechnology	sc-16566, RRID: AB_653287
β-actin	Sigma Aldrich	A1978, RRID: AB_476692
anti-rabbit horseradish peroxidase (HRP)-linked secondary antibody	GE Healthcare	NA934, RRID: AB_772206
anti-mouse horseradish peroxidase (HRP)-linked secondary antibody	GE Healthcare	NA931, RRID: AB_772210
CK7	RevMab Biosciences	31-1167-00, RRID: AB_2716482
CK20	Sigma Aldrich	HPA024309, RRID: AB_1852220
CDX2	Cell Signalling Technology	12306, AB_2797879
Biological samples		
Ascites	National Cancer Centre Singapore	N/A
Tumour specimen	National Cancer Centre Singapore	N/A
Chemicals, peptides, and recombinant proteins		
TM5441	Axon Medchem	2734
Tiplaxtinin	Selleckchem	S7922
Napabucasin	Selleckchem	S7977
BEZ235	Selleckchem	S1009
Mitomycin C	Kyowa Kirin	PL 16508
Critical commercial assays		
CellTitre-Glo assay	Promega	G7570
Allprep DNA/RNA/miRNA universal kit	Qiagen	80224
DNA Blood & Tissue mini kit	Qiagen	69504
SureSelect XT HS Target Enrichment kit and SureSelect Human All Exon v6 baits	Agilent Technologies	G9704K
Human phospho-receptor tyrosine kinase (RTKs) profiling	RayBiotech	AAH-PRTK-G1-4
Proteome profiler human cytokine array	R&D Systems	ARY022B
Human Serpin E1/PAI-1 Quantikine ELISA	R&D Systems	DSE100
Human IL-6 Quantikine ELISA Kit	R&D Systems	D6050
Human IL-10 Quantikine ELISA Kit	R&D Systems	D100B
Human CCL2/MCP-1 Quantikine ELISA Kit	R&D Systems	DCP00
Human MMP-9 Quantikine ELISA Kit	R&D Systems	DMP900
Total STAT3 ELISA	Cell Signalling Technology	7305C
p-STAT3 (Tyr705) ELISA	Cell Signalling Technology	7300C
Tumour Dissociation Kit, human	Miltenyi Biotec	130-095-929
10X Chromium Single Cell 3'GEM Kit	10X Genomics	PN-1000075
Bioanalyzer High Sensitivity DNA Kit	Agilent Technologies	5067-4626
Bradford protein assay	Bio-Rad	5000002

(*Continued on next page*)

Continued		
REAGENT or RESOURCE	SOURCE	IDENTIFIER
Deposited data		
Whole exosome sequencing data	This study	SRA: PRJNA781347
Data for microarray analysis and cytokine	This study	GEO: GSE189169
Additional Data	This study	Mendeley data: https://doi.org/10.17632/pt5mzwdwfz.1
Experimental models: Cell lines		
Colo-205	ATCC	CCL-222
SNU-C1	ATCC	CRL-5972
LP9/TERT-1	Brigham and Women's Hospital Cell Culture Core	CVCL_E108
HM-3/TERT	Brigham and Women's Hospital Cell Culture Core	CVCL_UZ42
CAF05	Neuromics	CAF05
CCD-18Co	ATCC	CRL-1459
Experimental models: Organisms/strains		
female BALB/c nude mice	Taconic Biosciences	C.Cg/AnNTac-Foxn1^{nu} NE9
Software and algorithms		
Harmonizome database		Rouillard et al.[50]
Kyoto Encyclopedia of Genes and Genomes (KEGG) pathway database		Kanehisa and Goto[51]
NCBI BioSystem database		Geer et al.[52]
TCGA database		https://www.cancer.gov/tcga
Kaplan-Meier plotter database		Nagy et al.[53]
10X Cell Ranger v6.0.1	10X Genomics	Zheng et al. [54]
Seurat v4.0		Stuart et al.[55]
Self-assembling manifolds (SAM) algorithm		Tarashansky et al.[56]
singleR (blueprint and ENCODE datasets)		Aran et al.[56]
HuGene-2_0-st	Affymetrix	Carvalho[57]
R (version 3.4.2)	R Foundation for Statistical Computing	https://cran.r-project.org/
Gene Set Enrichment Analysis (GSEA) software	Broad Institute	https://www.gsea-msigdb.org/gsea/index.jsp
BWA-MEM (version 0.7.17)		Li and Durbin[58]
SAMBLASTER (version 0.1.24)		Faust and Hall[59]
Sambamba (version 0.7.1)		Tarasov et al.[60]
Xenome (version 1.0.0)		Conway et al.[61]
Mutect2 (GATK version 4.0.12)	Broad Institute	https://gatk.broadinstitute.org/hc/en-us/articles/360037593851-Mutect2
Annovar		Wang et al.[62]

RESOURCE AVAILABILITY

Lead contact

Further information and requests for resources and reagents should be directed to and will be fulfilled by the lead contact, Chin-Ann Johnny Ong (johnny.ong.c.a@singhealth.com.sg).

Materials availability

There are restrictions to the availability of PDADX models as they are created with patient samples that are based in the National Cancer Centre Singapore. We are happy to collaborate with other researchers but will require a completed Project Agreement.

Data and code availability

- Whole exome sequencing data has been deposited at Sequence Read Archive (SRA) and are publicly available as of the date of production. Data for microarray analysis and cytokine has been deposited at Gene Expression Omnibus (GEO) and are publicly

available as of the date of production. Accession numbers are listed in the key resources table.Additional data has been deposited at Mendeley Data and are publicly available as of the date of production. The DOI is listed in the key resources table.

- All code used for the microarray analyses were written in R version 3.4.2 and will be made available from the corresponding author upon request.
- Any additional information required to reanalyse the data reported in this paper is available from the lead contact upon request.

EXPERIMENTAL MODEL AND SUBJECT DETAILS

Patient recruitment and biospecimen collection

A retrospective audit was performed for patients undergoing treatment for PC at National Cancer Centre Singapore from February 2003 and October 2019 (Table S1). Patients who were undergoing treatment for PC at National Cancer Centre Singapore were also prospectively identified and recruited for the study between June 2015 and January 2021 to validate the 3-biomarker prognostic panel in ascites and to stratify susceptible patients for PAI-1 inhibition. Demographic data can be found at Table S3 and Table S5. All patients provided written informed consent according to the study protocol as approved by the SingHealth Centralised Institutional Review Board (CIRB Ref: 2015/2479, 2018/3046 and 2020/2145). Ascitic fluid was collected from the peritoneal cavity at the beginning of cytoreductive surgery (CRS) or during routine paracentesis.

Cell lines

Colo-205 and SNU-C1, human colorectal cell lines representative of PC, were purchased from ATCC and cultured in RPMI-1640 with 10% FBS. LP9/TERT-1 and HM-3/TERT, human normal peritoneal mesothelial cell lines, were purchased from Brigham and Women's Hospital Cell Culture Core and cultured in M199/M106 with 15% iron-supplemented new-born calf serum, 0.4 μg/ml hydrocortisone and 10 ng/ml epidermal growth factor. CAF05, human colorectal tumour cancer-associated fibroblast, was purchased from Neuromics and cultured in VitroPlus III, low serum. CCD-18Co, human normal colonic fibroblast, was purchased from ATCC and cultured in EMEM with 10% FBS. All cell lines were supplemented with 100 U/ml penicillin, 100 μg/ml streptomycin and 1x antibiotic-antimycotic (Gibco) and were cultured at 37°C with 5% CO_2. All cells were serum starved for 24 hours prior to experiments.

Animals

All mice experiments were performed according to protocols approved by the SingHealth Institutional Animal Care and Use Committee (IACUC Ref: 2017/SHS/1295). A breeding pair of BALB/c nude mice (nomenclature: C.Cg/AnNTac-Foxn1^{nu} NE9) were purchased from Taconic Biosciences. All mice used in this study were 6-8 weeks old female BALB/c nude mice that were bred in-house and are sibling littermates. Mice were provided Teklad global 18% protein rodent diet (Envigo) and water *ad libitum*.

METHOD DETAILS

Processing of patient derived specimens and fluids

Ascitic fluids collected from recruited patients were subjected to centrifugation at 2,000 g for 10 minutes. The fluid component was then filter-sterilized using 0.22 μm filter and stored at -80°C for downstream analysis. The cellular component of ascites was used for generation of patient-derived ascites-dependent xenografts (PDADXs) and stored at -80°C in freezing medium (10% DMSO and 90% FBS) until further use. Tumour specimens harvested post-operatively were snap-frozen in liquid nitrogen immediately and stored at -80°C.

Clinical data extraction

Patient demographic and clinicopathological variables were obtained from the patients' electronic medical records. Cancer staging was determined by the American Joint Committee on Cancer (AJCC) manual 8th edition.[63] For patients with gynaecological cancers, the International Federation of Gynaecology and Obstetrics (FIGO) classification[64] was used. Peritoneal disease burden was assessed in patients who underwent surgical resection via the peritoneal carcinomatosis index (PCI) score,[65] and for those who underwent cytoreductive surgery, completeness of cytoreduction (CC) score was used to determine the resection status.

Proliferation assay

To assess the effect of ascites on proliferation, 5,000 Colo-205 and SNU-C1 cells/well were seeded in 96-well plate in triplicate and were grown in serum-free medium (SFM) supplemented with various concentration of cell-free ascites (CFA) as indicated. Cell proliferation was assessed at day 0 and day 5 using CellTitre-Glo assay (Promega) following the manufacturer's instructions. For *in vitro* drug treatment, 5,000 Colo-205 cells/well were seeded in 96-well plate in triplicate and were grown in SFM supplemented with 5% CFA (5% CFA medium) or SFM supplemented with 10% FBS (10% FBS medium) overnight, followed by treatment with 11 concentrations of various inhibitors (PAI-1 inhibitors: TM5441 and Tiplaxtinin, STAT3 inhibitor: Napabucasin, PI3K/mTOR inhibitor: BEZ235, DNA crosslinker: Mitomycin C) and DMSO vehicle for 72 hours. Cell viability after drug treatment was determined using CellTitre-Glo assay (Promega).

Cell migration assay

Colo-205 and SNU-C1 cells were pre-treated in three conditions: SFM, 10% FBS medium and 5% CFA medium for 24 hours. Pre-treated cells were then seeded into 6-well transwell migration assay at a density of 6 x 10^5 cells/well in triplicate. The inner chamber of the transwell was filled with SFM and the outer chamber was filled with 10% FBS medium as chemoattractant. Cells were allowed to migrate for 24 hours. Migrated cells were collected from medium in the outer chamber and the average of technical replicates was calculated.

Integrative multi-omics analysis

Integrative multi-omics analysis was performed to identify clinically relevant putative activators of STAT3 within ascites. In our initial interrogation process to identify biologically active ligands in ascites, we first curated proteins that were highly abundant in the 'peritoneal fluid' and 'ascites' datasets in the Harmonizome database.[50] By definition, peritoneal fluid refers to fluid in the intra-abdominal cavity in non-pathological states, while, ascites is the accumulation of fluid as a result of a pathological state. Top 10% proteins in each dataset as well as proteins shared in both databases were selected for further analysis. Next, STAT3-related genes were identified using the Kyoto Encyclopaedia of Genes and Genomes (KEGG) pathway database[51] and cross-referenced with the NCBI BioSystem database[52] to select for extracellular genes. The results from these 2 analyses were combined to derive a list of putative STAT3 activators that are secreted into ascites. To identify clinically and prognostically relevant STAT3 activators, we shortlisted the proteins via a two-step process. Only proteins that had existing inhibitors were considered. Subsequently, only proteins that were prognostically significant in at least three cancer subtypes in the following eight databases were selected; TCGA database[53] of colorectal cancer (n = 325) and ovarian cancer (n = 304) and Kaplan-Meier plotter database[66] of ovarian cancer (n = 1656), stomach adenocarcinoma (n = 371), bladder cancer (n = 404), lung cancer (n = 1925), lung squamous cell carcinoma (n = 495) and breast cancer (n = 1879).

Enzyme-linked immunosorbent assay (ELISA)

Levels of PAI-1 (DSE100), IL-6 (D6050), IL-10 (D1000B), CCL-2 (DCP00), and MMP-9 (DMP900) in CFA were measured using human Quantikine ELISA kits (R&D Systems). Total STAT3 and p-STAT3 (Tyr705) were measured by PathScan® Total Stat3 Sandwich ELISA Kit and PathScan® Phospho-Stat3 (Tyr705) Sandwich ELISA Kit (Cell Signalling Technology, 7305C and 7300C). All samples were performed with 2 technical replicates as per manufacturer's instructions. Foetal bovine serum (FBS) was used as control in all experiments because it had undetectable PAI-1 level and p-STAT3 (Tyr705) level below 0.2 (OD450).

Validation of prognostic secreted biomarkers via ELISA

Concentration of biomarkers in ascitic samples were determined via ELISA as described above and stratified by tertiles. Samples were characterized as having low expression (1-33%) or high expression (34-100%) of the biomarkers. We wanted to develop a robust panel that could be utilized easily with a binary outcome for each target (low or high). This stratification method has consistently been used in the literature and our team.[67–70] The prognostic abilities of the biomarkers were subsequently analysed via Kaplan-Meier plots and Cox proportional hazard regression model.

Single cell isolation, library preparation and sequencing

Four single-cell RNA-seq libraries were prepared from colorectal (two peritoneal tumours and ascites) and ovarian (ascites only) cancers from 2 individual patients. Tissues were dissociated into single cells using the Tumour Dissociation Kit, human (Miltenyi Biotec, Bergisch Gladbach, Germany) as per manufacturer's protocol. Ascites cells were cleared of red blood cells with 1X ammonium chloride lysis solution and washed with ice-cold phosphate buffered saline with 0.04% bovine serum albumin before downstream application. Each cell was captured and uniquely-barcoded using the 10X Chromium Single Cell 3'GEM Kit (PN-1000075) and 10X Chromium Controller according to manufacturer's protocol (10X Genomics, CA, USA). Briefly, an estimate of 16,000 cells were loaded at a concentration of 1200 cells/μl in an attempt to recover 10,000 cells. Following Gel Beads-in-emulsion (GEMs) generation, cell lysis and dissolution of the Gel Bead within each reaction vesicle enabled reverse transcription of polyadenylated mRNA, producing cDNA tagged with both a universal cell barcode and unique molecular index (UMI). The reaction vesicles were then lysed for cDNA amplification followed by purification using Silane magnetic beads. Quantification of cDNA was performed using Agilent Bioanalyzer High Sensitivity DNA Kit (Agilent Technologies, CA, USA). 25% of the total cDNA for each sample was carried forward for library preparation. Enzymatic fragmentation of the cDNA was carried out, followed by End-Repair and A-tailing, adaptor ligation and final library amplification PCR with unique sample indices for each sample. Final library quality was determined using the Agilent Bioanalyzer High Sensitivity DNA Kit. Insert sizes of the final libraries ranged between 430-480bp and were sequenced on Illumina Novaseq6000 platform with a target of 30,000 read pairs per cell at 150PE.

Analysis of single-cell sequencing data

The reads were demultiplexed and mapped against the hg38 reference genome using 10X Cell Ranger v6.0.1 (10X Genomics, CA, USA). Colorectal and ovarian cancers were analysed separately by loading the single-cell data into count matrices and merging the nodules and ascites using Seurat v4.0.[55] Cells which had less than 20% of transcripts mapping to mitochondrial genes were retained

for the scaling and log-normalization of their gene expression measurements. Self-assembling manifolds (SAM) algorithm,[71] an iterative soft feature selection strategy, was used to separate these cells with the default settings, and UMAP was used to visualize the distribution of these cells in the projection of significant principal components. These cells were then annotated with singleR[56] using the built-in transcriptomic reference (blueprint and ENCODE datasets). We removed 30 cells with ambiguous cell type annotation from the colorectal cancer case before final analysis. Within the peritoneal tumour nodules and ascites, differential expression analysis was respectively performed by comparing fibroblasts against all other cell types using the Wilcoxon rank-sum test, and the *p-value*s were adjusted for multiple hypotheses using the Bonferroni correction.

Conditioned medium collection

To quantify basal secretion of PAI-1 contributed by various cell types in PC, PC cell lines (Colo-205 and SNU-C1) and stromal cell lines (LP9/TERT-1, HM-3/TERT, CAF05 and CCD-18Co) were seeded at 5 x 10^5 cells in 5 ml complete medium in T25 flasks overnight in duplicate. Following this, cells were serum starved for 24 hours and the medium was replaced with fresh complete medium and incubated for 24 hours. All conditioned medium (CM) was collected, centrifuged to remove cellular debris, filtered with 0.22 μm filter and stored at -80°C until assayed. PAI-1 levels in CMs were quantified by ELISA.

RNA microarray and analysis

To identify signaling pathways upregulated upon treatment with ascites, Colo-205 and SNU-C1 cells were treated with 5% and 0.1% colorectal PC CFA medium (n = 2) for 24 hours. To identify signaling pathways affected by PAI-1 inhibition, Colo-205 cells were treated with CFA representative of PPA group, CAP group or FBS (control) in the presence of DMSO vehicle or 27.25 μM TM5441 (TM5441 IC_{50} of PC085 CFA-treated Colo-205) for 24 hours. Total RNA was isolated using Qiagen Mini Kit (Qiagen) following the manufacturer's instructions. Gene expression profiling was performed using Affymetrix HuGene-2_0-st[57] (Affymetrix). Microarray data was uploaded into the free programming software R (version 3.4.2) for processing and normalization. Gene Set Enrichment Analysis (GSEA) was performed using GSEA software[72] (Broad Institute).

Whole exome sequencing and analysis

Genomic DNA from tissues and blood was isolated using Allprep DNA/RNA/miRNA universal kit (Qiagen, #80224) and DNA Blood & Tissue mini kit (Qiagen, #69504) respectively in accordance to manufacturer's guidelines. Whole exome sequencing was performed using the SureSelect XT HS Target Enrichment kit and SureSelect Human All Exon v6 baits (Agilent Technologies, #G9704K). Library was sequenced at 200X coverage on an Illumina Novaseq 6000 platform for 150 paired-end sequencing. Raw FASTQ files from the sequencing facility were aligned to the human reference genome (hs37d5) using BWA-MEM[58] (version 0.7.17). Aligned reads underwent duplicate marking using SAMBLASTER[59] (version 0.1.24) and were then sorted using Sambamba[60] (version 0.7.1). Prior to alignment, FASTQ files from xenografts were pre-processed using Xenome[61] (version 1.0.0) to remove reads mapping to the host mouse genome (mm9). Somatic mutation calling was then performed on the BAM alignment files using Mutect2 (GATK version 4.0.12), with the patient blood sample as the normal sample. Variants from Mutect2 were filtered using the FilterMutectCalls command, and then annotated using Annovar.[62] Somatic mutations in genes identified in patient tumour samples were examined in ascites cell pellet and in PDADX tumour samples to compare their variant allele frequencies.

Human phospho-receptor tyrosine kinase (RTKs) profiling

Human phospho-receptor tyrosine kinase (RTKs) profiling (RayBiotech, AAH-PRTK-G1-4) consisting of 71 RTKs was used to analyse common RTKs activated in PC cell lines upon treatment with ascites. Colo-205 and SNU-C1 cells were treated with 5% colorectal PC CFA medium (n = 2) and 10% FBS medium (control) for 24 hours. Total protein concentration was determined with Bradford protein assay (Bio-Rad) and 40 μg of protein per sample was used for phospho-RTKs profiling following the manufacturer's instructions.

Human cytokine profiling

Proteome profiler human cytokine array (R&D Systems, ARY022B) consisting of 105 cytokines was used to profile malignant CFA from patients with colorectal PC (n = 4) and benign CFA from patient with benign serous cystadenofibroma (n = 1). Concentration of proteins in all ascitic fluids was quantified with Bradford protein assay (Bio-Rad) and equal amount of proteins were incubated with the membrane array according to the manufacturer's instructions. Supervised and unsupervised clustering of proteomics data was performed using the 'gplots' package in R (version 3.6.0).[73]

Assessment of STAT3 activity in PC cells

To assess STAT3 activation in PC cells upon treatment with ascites, proteins were isolated from cell lysates of Colo-205 and SNU-C1 cells treated with 5% CFA medium for 24 hours. To assess effect of PAI-1 inhibition on STAT3 activation, proteins were isolated from cell lysates of Colo-205 cells treated with 5% CFA medium and various concentrations of TM5441 for 8 hours. In all experiments, 25 μg of protein was used for total STAT3 and p-STAT3(Tyr705) ELISA. All samples were performed with 2 technical replicates as per manufacturer's instructions.

Protein lysate preparation and western blot

To assess STAT3 and JAKs activation in PC cells upon treatment with ascites, Colo-205 and SNU-C1 cells were treated with SFM, 10% FBS medium, 0.1% CFA medium and 5% CFA medium for 24 hours. To determine the effect of PAI-1 inhibition on STAT3 activation, SNU-C1 cells were treated with 5% PPA CFA medium and various concentration of TM5441 as indicated or DMSO vehicle for 8 hours. All harvested cells were lysed with M-PER reagent and supplemented with Pierce protease and phosphatase inhibitor (Thermo Scientific). Total protein concentrations were determined using Bradford protein assay (Bio-Rad). Amount of proteins used were: 5 μg for total STAT3 and β-actin, 25 μg for p-STAT3 (Tyr705) and p-STAT3 (Ser727), 10 μg for JAK1, JAK2, p-JAK1 (Tyr1022/Tyr1023) and p-JAK2 (Tyr1007/Tyr1008). Lysates were denatured at 97°C for 5 minutes and resolved in 10% polyacrylamide gels in Tris/glycine/SDS running buffer (24.76 mM Tris, 191.83 mM glycine and 0.1% SDS) followed by transfer to 0.45 μm nitrocellulose membrane (Bio-Rad) in Tris/glycine/methanol transfer buffer (24.76 mM Tris, 191.83 mM glycine and 20% methanol). The membranes were blocked with 5% non-fat milk in 1x PBS containing 0.1% Tween 20 (PBST) for 1 hour at room temperature before blotting with primary antibodies for 1.5 hours. Dilutions of the primary antibodies used were: 1:2,000 for total STAT3, 1:1,000 for p-STAT3 (Tyr705), p-STAT3 (Ser727), JAK1, p-JAK1 (Tyr1022/Tyr1023), JAK2, p-JAK2 (Tyr1007/Tyr1008), and 1:2,000 for β-actin. After 4 washes (5 min per wash) in PBST, the blots were incubated with anti-rabbit (NA934) or anti-mouse (NA931) horseradish peroxidase (HRP)-linked secondary antibody (GE Healthcare) for 30 minutes at room temperature. After another 4 washes in PBST, membranes were incubated with SuperSignal West Dura substrate (Thermo Scientific) for 5 minutes and subsequently exposed to autoradiography film (Santa Cruz Biotechnology). Images were scanned using GS-800 TM calibrated densitometer (Bio-Rad).

Patient-derived ascites-dependent xenografts (PDADXs) generation

Ascites collected from patients with PC were centrifuged at 2,000 g for 10 minutes to concentrate the cellular component and to separate the fluid component. 1 ml of cell pellet was resuspended with 1 ml of ascitic fluid and 400 μl of the mixture was implanted intraperitoneally into 6-week-old BALB/c nude mouse (female, $n = 5$ mice) to generate PDADX passage 0 (P0). PDADXs tumour formation for P0 were generally observed 6-months to 1-year post-implantation.

Immunohistochemical (IHC) staining

Formalin-fixed paraffin-embedded (FFPE) specimens from PDADX tumours were characterized using chromogen-based immunohistochemical (IHC) staining. All IHC staining was carried out using the Bond Max Autostainer (Leica Microsystems) as per the manufacturer's recommendations. FFPE blocks were sectioned into 4 μm sections, mounted on slides, and probed with antibodies against CK20, CK7 and CDX2 to confirm the histology and origin of PDADX tumours formed. Rabbit monoclonal anti-CK7 (RevMab Biosciences, #31-1167-00, 1:200, pH 9, 20 minutes), rabbit polyclonal anti-CK20 (Sigma Aldrich, HPA024309, 1:200, pH 9, 20 minutes) and rabbit monoclonal anti-CDX2 (Cell Signalling Technology, #12306, 1:100, pH 9, 20 minutes) were used in the staining.

In vivo PC cell line mouse model drug treatment

To determine the efficacy of PAI-1 inhibition in ascites subgroups with different susceptibility *in vivo*, 5 x 10^6 of Colo-205 cells were co-injected with CFA representative of PAI-1 paracrine addicted (PPA) group, co-activators predominant (CAP) group or FBS (control) into abdominal cavity of 6- to 8-week-old BALB/c nude mice (female, $n = 5$ mice/group) and treated with 1.75 mM TM5441 administered intraperitoneally. Ascites and drug treatment were performed by injecting 400 μl of 5% CFA or 10% FBS with TM5441 in PBS intraperitoneally every 3 days for 21 days. To determine the optimal drug concentration and drug delivery method, 6- to 8-week-old female BALB/c nude mice ($n = 16$) was injected intraperitoneally with 5 x 10^6 of Colo-205 cells per mouse. The mice were divided into 4 groups and given the following treatments: (i) 5% CFA with 1% DMSO, (ii) 5% CFA with 1 mM TM5441, (iii and iv) 5% CFA with 2 mM TM5441. Treatment was performed by injecting 400 μl of 5% CFA with DMSO vehicle/drug in PBS intraperitoneally (i – iii) and orally (iv) every 3 days, up to 21 days. In both experiments, mice were sacrificed after 3 weeks of ascites and drug treatment. Tumour burden was quantified based on a modified peritoneal carcinomatosis index (PCI) score and presented as total PCI score. Total PCI score was calculated based on the sum of score for each region and ranges from 0 to 39 (Figure S7).

PAI-1 inhibition of PDADX generated from matched ascites

Matched patient's CFA and its cellular components were used to generate PDADXs to better recapitulate PC patients. PDADX tumours (100 mg/mouse) were implanted into female BALB/c nude mice intraperitoneally. Using PDADX models generated from two representative PC patients, the following treatments were conducted: (i) 5% matched CFA with 1% DMSO, (ii) 5% matched CFA with 2 mM TM5441, (iii) 10% FBS with 1% DMSO and (iv) 10% FBS with 2 mM TM5441. Ascites and drug treatment were performed via intraperitoneal administration every 3 days for 21 days. Tumour burden was quantified by weighing all visible tumours after mice were sacrificed.

PAI-1 inhibition of CAP PDADX in the presence of matched versus non-matched ascites

To determine if susceptibility to PAI-1 inhibition is reliant on paracrine factors in ascites and not tumours, CAP PDADX (whose patient's CFA are not responsive to PAI-1 inhibition) was treated with PPA CFA. CAP PDADX tumours (100 mg/mouse) were implanted into 16 female BALB/c nude mice intraperitoneally. The mice were divided into 4 groups and given the following treatment: (i) 5% CAP

CFA with 1% DMSO, (ii) 5% CAP CFA with 2 mM TM5441, (iii) 5% PPA CFA with 1% DMSO, and (iv) 5% PPA CFA with 2 mM TM5441. Ascites and drug treatment were performed via intraperitoneal administration every 3 days for 21 days. Tumour burden was quantified by weighing all visible tumours after mice were sacrificed.

QUANTIFICATION AND STATISTICAL ANALYSIS

Clinical endpoint and statistical analysis

The primary clinical endpoint was overall survival (OS), defined as the time from CRS or time of ascites collection to death, regardless of cause. Presence of ascites was defined by an accumulation of more than 200 ml fluid in the abdominal cavity. OS in The Cancer Genome Atlas (TCGA) and Kaplan-Meier plotter data was defined as the time from diagnosis to death, regardless of cause. Survival outcome was analysed by Kaplan-Meier analysis and log-rank test. Univariate and multivariable Cox proportional hazard regression models were used to examine the association of various factors with OS. The final model was built by fitting factors that were $P < 0.1$ on univariate analysis, excluding individual biomarkers, into a backward stepwise Cox regression multivariate model (entry probability at 0.05 and removal probability at 0.10). Factors that remained statistically significant in this multivariable model were considered prognostic. The association between categorical variables was analysed by Chi-square. Correlation between continuous data was examined using Pearson's correlation coefficient. Statistical analysis between groups was performed using unpaired two-sided t-test. The *P* values for gene set enrichment analysis were generated using GSEA software. Statistical analyses were performed using IBM SPSS Statistics (version 25.0) and GraphPad Prism (version 7.0e). The statistical significance level was set at $P < 0.05$.